

# VANISHING FRACTALITY: A DETERMINISTIC, ENDOGENOUS, NON-STATIONARY $S$ -ADIC AUTOMATON FOR THE SIEVE OF ERATOSTHENES

BIRKE HEEREN 

**ABSTRACT.** We present a deterministic, endogenous, non-stationary  $S$ -adic automaton that models the Sieve of Eratosthenes as a dynamical system over a finite symbolic alphabet. The automaton operates through three operators — shift, expansion, and filtering — applied sequentially to a growing symbolic tape, and provably reproduces the classical prime-composite classification for every integer  $n \geq 2$ . Unlike algorithmic sieves, the automaton generates an internal symbolic representation of the number line whose structure can be analyzed at every step.

*Our first focus is: Can this new framework reproduce known mathematical knowledge?*

We demonstrate that this representation is not arbitrary: the tape exhibits a four-letter substructure  $\{a, b, c, d\}$  governed by an explicit substitution morphism and upper triangular transition matrix  $M_p$ . The dominant eigenvalue  $p - 2$  controls the population dynamics of twin prime templates, yielding a recursive growth formula consistent with OEIS sequence A059861 and consistent with the combinatorial factors underlying the Hardy-Littlewood  $k$ -tuple conjecture.

A central structural result is the Stability Zone  $[n + 1, 2n - 1]$ , a provably immutable interval in which prime candidates survive all prior filtering steps. Using a Frozen Window technique, we verify the persistence of symbolic structure experimentally up to  $n = 250,000$ .

*Our second focus is: Can this new framework lead to new mathematical knowledge?*

Finally, we discuss a new way of fractal dimension (self similarity), fitting for the prime candidate set within the Stability Zone. It begins near 0.92 and increases toward 1 as  $n \rightarrow \infty$ , following  $D = \ln(p - 1)/\ln(p)$ . This process — vanishing fractality — unfolds dynamically inside the growing, advancing Stability Zone as it travels through the number line, and provides a structural perspective on the transition from the ordered structure of small primes to the apparent randomness observed in large-scale prime distributions.

The automaton is offered not as a computational tool for generating primes, but as a research instrument: a symbolic framework in which arithmetic properties of the natural numbers emerge from the internal dynamics of the system.

## CONTENTS

1. Introduction	3
1.1. Related Work	4

---

2020 *Mathematics Subject Classification.* 11N05, 11B85, 37B10, 68Q45, 28A80.

*Key words and phrases.* Sieve of Eratosthenes; prime numbers; symbolic dynamics;  $S$ -adic systems; substitution morphisms; deterministic automata; fractal dimension; vanishing fractality; twin prime conjecture; Stability Zone; transition matrix; Hardy-Littlewood conjecture; non-stationary dynamical systems; primorial; Hydra effect.

Corresponding author. E-mail: birke.heeren@uni-rostock.de | ORCID: <https://orcid.org/0000-0001-6713-583X>.

1.2. Organization of the Paper	5
2. Topic	6
2.1. Topic: A Symbolic Research Instrument for the Sieve of Eratosthenes	6
3. The Automaton	7
3.1. Symbolic Domains	7
3.2. Structure of the Automaton	8
3.3. Operators	10
3.4. Transition Function	10
3.5. Note on the Binary Tape	11
3.6. Illustrative Example: First Five Steps	11
4. Synchronization and Equivalence to the Sieve of Eratosthenes	12
4.1. Synchronization	12
4.2. Equivalence to the Sieve of Eratosthenes	13
4.3. Width of the Tape	13
5. The Four-Letter Substructure	14
5.1. Emergence of the Substructure	14
5.2. Structural Interpretation	15
5.3. Stability of the Substructure	16
5.4. Transition Rules	16
5.5. Lemma on Three Consecutive Primes	17
6. Substitution Morphisms, Transition Matrix, and the Hydra Effect	18
6.1. Substitution Morphisms	18
6.2. Transition Matrix	19
6.3. The Hydra Effect	19
6.4. Connection to OEIS A059861 and Hardy–Littlewood	20
6.5. Normalized Transition Matrix and Asymptotic Densities	21
6.6. Hierarchical Renormalization: The Emergent Letter $e$	21
7. The Stability Zone	22
7.1. Definition and Motivation	22
7.2. Proof of Immutability	22
7.3. Advancement of the Stability Zone	23
7.4. Confirmed Primes in the Stability Zone	23
7.5. Visual Representation	23
7.6. Analogy to the Prime Number Theorem	24
8. The Frozen Window Experiment	25
8.1. Motivation and Computational Challenge	25
8.2. The Frozen Window Technique	25
8.3. Validity of the Frozen Window	26
8.4. Termination and Validity of the Algorithm	27
8.5. Boundary Conditions of the Letter Count	27
8.6. Implementation	28
8.7. Results	28
8.8. Limitations and Scope	29
9. Vanishing Fractality	30

9.1. Motivation	30
9.2. The Prime Candidate Set as a Cantor-Type Structure	30
9.3. The Local Fractal Dimension	31
9.4. The Cumulative Fractal Dimension	31
9.5. The Stability Zone Dimension and Its Relationship to the Full Tape	33
9.6. Vanishing Fractality	34
9.7. Experimental Confirmation	35
10. Conclusion	36
10.1. Summary of Results	36
10.2. The Automaton as a Research Instrument	38
10.3. What Remains Open	38
10.4. Code and Data Availability	39
10.5. Closing Remark	39
Declaration of AI-Assisted Tools	39
Funding and Project History	39
Acknowledgements	40
References	40

## 1. INTRODUCTION

The distribution of prime numbers stands as one of the central unsolved problems in mathematics. Despite centuries of analytic progress — from the Prime Number Theorem to the Riemann Hypothesis — the local structure of the primes remains resistant to closed-form description. Statistical models and probabilistic heuristics, such as the Cramér model [8] and the Hardy–Littlewood conjectures [15], capture the large-scale behavior of prime gaps and prime constellations with remarkable accuracy. Yet they offer no deterministic explanation for why individual primes fall where they do.

This paper adopts a different perspective. We do not ask what primes look like statistically. We ask what kind of dynamical system generates them — and what that system reveals about their structure.

We present a deterministic, endogenous, non-stationary  $S$ -adic automaton whose internal state evolves through three operators: a shift  $S_n$ , an expansion  $X_n$ , and a filter  $F_n$  (see Figure 3). The automaton maintains a cyclic symbolic tape over the binary alphabet  $\Sigma_{\text{CP}} = \{L, M\}$  and processes one natural number per step. No external primality test is required: the classification of a number as prime or composite emerges from the symbolic state of the tape at the moment of encoding. The automaton is provably equivalent to the Sieve of Eratosthenes in the sense that it produces exactly the same classification of every integer  $n \geq 2$ .

What distinguishes the automaton from the classical sieve is not what it computes, but what it records. At every step, the tape carries a complete symbolic representation of the number line — periodic, structured, and analytically accessible. This representation is the research tool we offer Figure 1.

Analysis of the tape reveals a four-letter substructure  $\{a, b, c, d\}$  defined over blocks of width 6, governed by an explicit substitution morphism and a prime-dependent transition



Classical constructions such as the Sieve of Eratosthenes [10] provide a procedural method for identifying primes by iteratively removing multiples. More advanced sieve methods, including Brun’s sieve and later developments summarized in Halberstam and Richert [14], extend this approach to deeper analytic questions concerning prime distribution.

The Hardy–Littlewood conjectures [15] extend probabilistic reasoning to prime constellations, predicting the density of twin primes and more general  $k$ -tuples through singular series involving products over primes. These conjectures remain unproven, and no deterministic framework has yet provided a constructive account of the combinatorial factors they involve.

From an entirely different direction, the theory of symbolic dynamics and  $S$ -adic systems has developed powerful tools for analyzing sequences generated by substitution morphisms over finite alphabets. Foundational treatments are given by Lind and Marcus [18] and Allouche and Shallit [1], while the non-stationary generalization to  $S$ -adic systems is developed by Fogg [12] and Berthé and Delecroix [4]. These frameworks have been applied to a wide range of combinatorial and arithmetic sequences, but the classical Sieve of Eratosthenes has not previously been formulated as a deterministic symbolic dynamical system with an explicit internal state evolution.

Connections between number theory and fractal geometry have been explored by Lapidus and van Frankenhuysen [16], where zeta functions and complex dimensions provide a geometric framework for understanding number-theoretic structures. Our perspective complements this classical framework by providing a structural model in which arithmetic properties emerge from symbolic dynamics.

This paper bridges these directions. The automaton connects sieve theory with symbolic dynamics and non-stationary  $S$ -adic systems, offering a new perspective on the generation of prime numbers in which fractal geometry emerges endogenously from the sieving process itself.

A related but independent approach to primality without divisibility has been developed by Bilokon [5], who introduces an imbalance metric  $\delta(p, q) = |p - q|/(p + q)$  on integer pairs and a Möbius transformation of this metric. In that framework, primality corresponds to a novelty condition: primes are exactly those integers that introduce new conjugate imbalance values not previously encountered. Bilokon’s Proposition 5 establishes that the order in which new imbalance denominators appear is entirely deterministic, governed by the permutation A006369. This deterministic structure parallels the endogenous, non-divisibility-based generation of primes in our automaton, where primality emerges from the binary state of the tape rather than from divisibility testing. The two frameworks are complementary: Bilokon’s approach operates in a Möbius-transformed rational metric space, while ours operates in a symbolic dynamical system over a binary alphabet.

**1.2. Organization of the Paper.** The paper is organized as follows. Section 2 states the main topic. Section 3 defines the automaton and its operators. Section 4 establishes the synchronization between the tape and the natural numbers and proves equivalence to the Sieve of Eratosthenes. Section 5 develops the four-letter substructure and its substitution morphisms. Section 6 analyzes the transition matrix  $M_p$ , the Hydra Effect and the hierarchical renormalization of further substructures. Section 7 introduces the Stability Zone. Section 8 presents the Frozen Window experiment. Section 9 derives the fractal dimension and establishes vanishing fractality. Section 10 concludes.

At the end of the paper, we provide a full bibliography and a declaration of AI-assisted tools used during preparation and acknowledgments.

## 2. TOPIC

**2.1. Topic: A Symbolic Research Instrument for the Sieve of Eratosthenes.** The automaton  $\mathcal{A}$  is not proposed as an efficient algorithm for generating primes, but as a *symbolic research instrument*: a deterministic, endogenous dynamical system whose internal state provides a geometric and spectral observatory for arithmetical phenomena arising from the sieve of Eratosthenes. There exists a deterministic, endogenous, non-stationary  $S$ -adic automaton

$$\mathcal{A} = (N, E, CP; S_n, X_n, F_n)_{n \geq 1}$$

that can be used as a new research tool and bridges different areas of mathematics.

Properties and examples of what this tool is useful for:

- (i) **Endogenous evolution without divisibility tests.** At step  $n$ , the state of  $\mathcal{A}$  consists of two single-cell registers  $N_n \in \mathbb{N}$  and  $E_n \in \Sigma_E = \{\text{ONE}, P, M\}$ , together with a cyclic binary tape  $CP_n \in \{L, M\}^{w_n}$ . The update from step  $n - 1$  to step  $n$  is given by a fixed composition of three operators

$$CP_n = \begin{cases} F_n(X_n(S_n(CP_{n-1}))) & \text{if } E_n = P, \\ S_n(CP_{n-1}) & \text{if } E_n = M, \end{cases}$$

where  $S_n$  is a cyclic shift by one cell,  $X_n$  is an  $n$ -fold expansion, and  $F_n$  is an  $n$ -stride filter marking multiples as  $M$ . No external primality test or divisibility operation is ever applied; primality information emerges solely from the internal binary tape. In particular,

$$E_n = \begin{cases} \text{ONE} & \text{if } n = 1, \\ P & \text{if } CP_{n-1}[1] = L, \\ M & \text{if } CP_{n-1}[1] = M, \end{cases}$$

so that  $E_n$  is determined entirely by the symbolic state of  $\mathcal{A}$ .

- (ii) **Exact equivalence to the classical Sieve of Eratosthenes.** For every integer  $n \geq 2$ , the automaton  $\mathcal{A}$  produces the same prime/composite classification as the classical sieve:

$$n \text{ is prime} \iff CP_{n-1}[1] = L, \quad n \text{ is composite} \iff CP_{n-1}[1] = M.$$

Thus  $\mathcal{A}$  is not a heuristic model: it reproduces the sieve deterministically and point-wise on  $\mathbb{N}$ .

- (iii) **Full symbolic recording of the sieve state.** At every finite step  $n$ , the tape  $CP_n$  is a strictly periodic binary word whose length equals the primorial of the largest prime  $p \leq n$ :

$$|CP_n| = \prod_{p \leq n} p$$

State space: The tape encodes the entire sieve state at level  $n$  as a geometric object: each cell records whether the corresponding residue class modulo the primorial has been eliminated ( $M$ ) or survives as a prime candidate ( $L$ ). In this sense,  $\mathcal{A}$  does not merely *compute* the sieve output; it *records* a complete symbolic snapshot of the sieve

as it unfolds. This representation turns the sieve from a purely procedural elimination process into a structured state space, making its internal configuration accessible to geometric, symbolic, and spectral analysis.

- (iv) **Emergent finite-alphabet geometry.** From step  $n = 4$  onward, the tape  $CP_n$  decomposes canonically into blocks of length 6, and only four such blocks ever occur:

$$a = \langle LMLMMM \rangle, \quad b = \langle LMMMMM \rangle, \quad c = \langle MMLMMM \rangle, \quad d = \langle MMMMMM \rangle.$$

These blocks form a second-order alphabet  $\Sigma^{(2)} = \{a, b, c, d\}$  with clear arithmetic meaning:  $a$  is the twin-prime template,  $b$  and  $c$  are single prime candidates, and  $d$  encodes six consecutive composites. The evolution of  $\Sigma^{(2)}$  under  $\mathcal{A}$  is governed by an explicit prime-dependent  $S$ -adic substitution  $\sigma_p : (\Sigma^{(2)})^* \rightarrow (\Sigma^{(2)})^*$  and its upper triangular transition matrix  $M_p$ , whose dominant eigenvalue  $p - 2$  controls the population dynamics of twin-prime templates.

- (v) **Built-in stability zone and fractal viewpoint.** For each step  $n$ , there is a canonical *Stability Zone*

$$SZ_n = [n + 1, 2n - 1]$$

in which the symbolic information on the tape is provably immutable under all previous filtering steps. Within  $SZ_n$ , the surviving prime candidates form a Cantor-type subset Figure 2 with local scaling ratio  $(p - 1)/p$  at prime level  $p$ , giving a natural notion of “local fractal dimension”

$$D(p) = \frac{\ln(p - 1)}{\ln(p)},$$

which increases to 1 as  $p \rightarrow \infty$ . This yields a deterministic, geometric account of how the highly structured regime of small primes transitions into the apparent randomness of large-scale prime distributions.

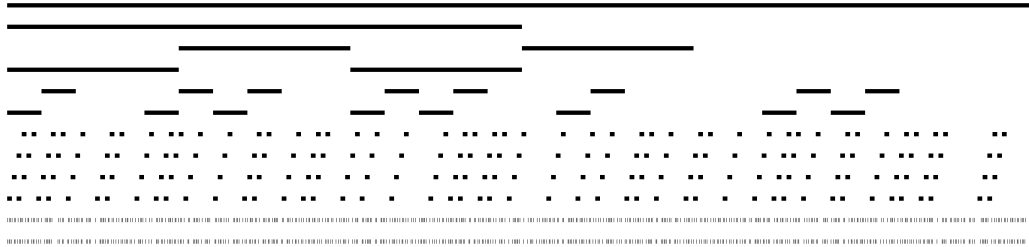


FIGURE 2. The Cantor-type dust of the L symbols on tape  $CP_n$ .

### 3. THE AUTOMATON

**3.1. Symbolic Domains.** The automaton operates over three distinct symbolic domains, one for each of its three components.

**Register  $N$**  holds natural numbers. It carries no symbolic alphabet — its state at step  $n$  is simply the natural number  $n$ , generated by the successor operation (Peano [22]). The mapping between automaton steps and  $\mathbb{N}$  is the identity.

**Register**  $E$  holds the qualitative encoding of the current natural number. Its alphabet is:

$$(1) \quad \Sigma_E = \{\text{ONE}, P, M\}$$

The three symbols correspond to the three arithmetically distinct categories of natural numbers: ONE marks the number 1, which is neither prime nor composite;  $P$  marks a prime; and  $M$  marks a composite. These three categories are exhaustive and mutually exclusive, and no symbol can be removed without losing the ability to distinguish them.

**Tape** CP carries a symbolic representation of the number line. Its alphabet is strictly binary:

$$(2) \quad \Sigma_{\text{CP}} = \{L, M\}$$

The symbol  $L$  (live) marks a position that has not yet been identified as composite — it is a prime candidate. The symbol  $M$  (multiple) marks a position that has been identified as composite by a prior filtering step. The binary alphabet is minimal and sufficient: the tape needs only to distinguish surviving candidates from eliminated ones.

This separation of symbolic domains reflects the actual structure of the system. The tape never carries primality information directly — it carries only the binary record of which positions have been eliminated. Primality is determined by Register  $E$ , which reads the tape but is not part of it.

**3.2. Structure of the Automaton.** The automaton  $\mathcal{A}$  consists of two single-cell registers and one symbolic tape.

**Register**  $N$  evolves by the Peano successor operation [22]:

$$(3) \quad N_n = N_{n-1} + 1, \quad \text{with } N_1 = 1.$$

**Register**  $E$  holds the encoding of the current number  $n$ . At each step, the encoding function  $\mu_n$  reads the first symbol of the tape and assigns:

$$(4) \quad E_n = \begin{cases} P & \text{if } \text{CP}_{n-1}[1] = L \\ M & \text{if } \text{CP}_{n-1}[1] = M \end{cases}$$

Note that  $E_n = \text{ONE}$  is assigned only at the initial step  $n = 1$ , where  $\text{CP}_1[1] = L$  by initialization but  $N_1 = 1$  is treated separately. For all  $n \geq 2$ , the encoding is fully determined by equation (4).

No external primality test is required at any point. Whether the current number is prime or composite is determined entirely by the binary state of the tape at that moment —  $L$  or  $M$  at position  $\text{CP}_{n-1}[1]$ .

**Tape** CP begins with a single cell and grows over the course of the automaton's evolution. The leftmost cell is denoted  $\text{CP}_n[1]$  and the rightmost cell is denoted  $\text{CP}_n[\text{last}]$ . New cells are appended exclusively to the right end of the tape. At every finite step  $n$ , the tape carries a strictly periodic word over  $\Sigma_{\text{CP}} = \{L, M\}$  — that is, a word that repeats exactly with no drift. The width of the tape at step  $n$  equals the primorial of the largest prime  $p \leq n$ :

$$(5) \quad |\text{CP}_n| = \prod_{p \leq n} p$$

where the product runs over all primes  $p$  less than or equal to  $n$ . The tape grows only at prime steps. At composite steps the width remains unchanged.

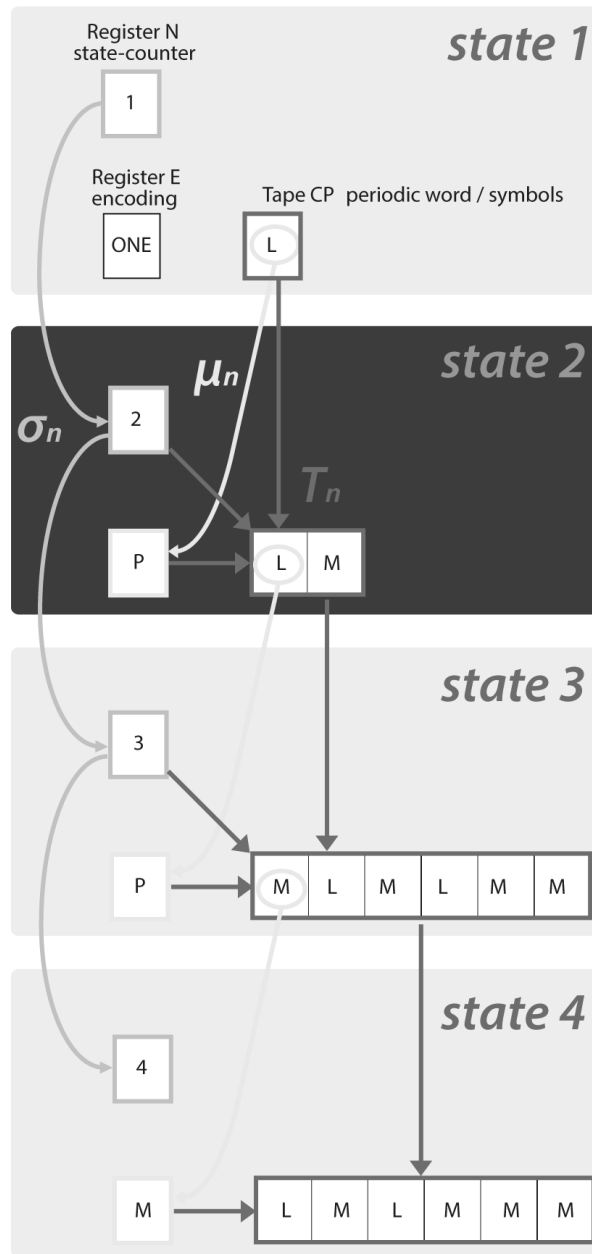


FIGURE 3. Dynamic development of the non-stationary  $S$ -adic system. The automaton evolves through four states, showing Register  $N$  (state counter), Register  $E$  (encoding), and Tape CP (binary periodic word). At state 2, the first prime  $n = 2$  triggers the expansion operator  $X_n$  and filter operator  $F_n$ , growing the tape from width 1 to width 2. The three symbolic domains  $\mathbb{N}$ ,  $\Sigma_E = \{\text{ONE}, P, M\}$ , and  $\Sigma_{CP} = \{L, M\}$  are visually distinct.

**3.3. Operators.** The evolution of the tape is governed by three operators. Each operator acts exclusively on the binary tape alphabet  $\Sigma_{CP} = \{L, M\}$ .

**Shift operator  $S_n$ .** The first cell  $CP[1]$  is removed from the left end of the tape and appended to the right end, becoming the new  $CP[\text{last}]$ . This is a cyclic rotation Figure 4 by one position. It keeps Register  $N$  and the tape in lockstep: after the shift, the symbol at position  $CP_n[1]$  corresponds to the natural number  $n + 1$ . The shift is applied at every step, whether  $n$  is prime or composite.

**Expansion operator  $X_n$ .** Applied only when  $E_n = P$ . The full tape is copied and  $n - 1$  additional copies are appended to the right end, so that the new tape consists of exactly  $n$  concatenated copies of the previous tape. The expansion multiplies the period length by  $n$  but does not alter the relative positions of  $L$  and  $M$  symbols within the period. No new binary configurations are introduced — the existing pattern is replicated exactly. The width of the tape after expansion is  $n \cdot |CP_{n-1}|$ , see Figure 6.

**Filter operator  $F_n$ .** Applied only when  $E_n = P$ . The operator traverses the tape with step size  $n$ , visiting every  $n$ -th cell beginning at position  $n$ , and replaces every  $L$  encountered with  $M$ , leaving existing  $M$  symbols unchanged. In this way, all multiples of  $n$  within the tape are marked as composite. The filter does not change the width of the tape. It acts only on the binary symbol  $L$  — it has no effect on positions already marked  $M$ .

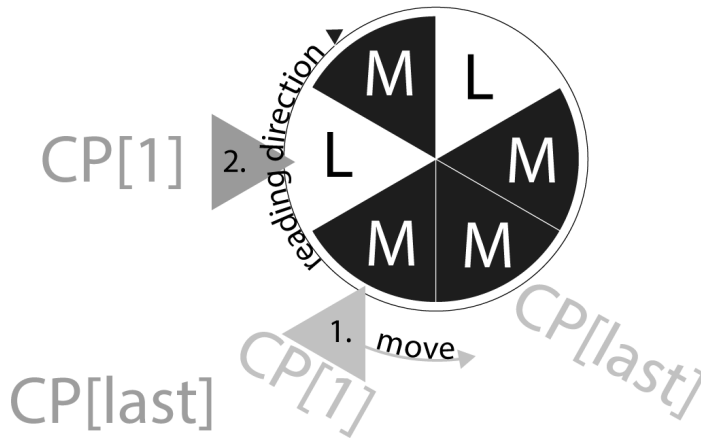


FIGURE 4. The tape  $CP_n$  displayed as a cyclic structure. The shift operator  $S_n$  rotates the tape by one position, moving the symbol at  $CP[1]$  to  $CP[\text{last}]$  and advancing the reading head to the next symbol. This cyclic rotation preserves the strict periodicity of the tape and keeps Register  $N$  and  $CP_n$  in lockstep.

**3.4. Transition Function.** The complete transition of the tape at step  $n$  is:

$$(6) \quad CP_n = \begin{cases} F_n(X_n(S_n(CP_{n-1}))) & \text{if } E_n = P \\ S_n(CP_{n-1}) & \text{if } E_n = M \end{cases}$$

The initial state of the system is  $N_1 = 1$ ,  $E_1 = \text{ONE}$ , and  $CP_1 = \langle L \rangle$ .

When  $E_n = P$ , the three operators are applied in strict order: first  $S_n$ , then  $X_n$ , then  $F_n$ . The order is not arbitrary and cannot be changed without altering the output. The shift must precede the expansion so that the tape is correctly aligned with the current number before replication. The filter must follow the expansion so that all  $n$  copies of the tape are marked consistently — applying the filter before expansion would leave  $n - 1$  copies of the tape unfiltered.

**3.5. Note on the Binary Tape.** The choice of a binary alphabet  $\Sigma_{CP} = \{L, M\}$  for the tape is not merely a notational convenience. It reflects a structural fact: the tape encodes exactly one binary decision for each position — eliminated or not yet eliminated. This minimality has two consequences that will become important in later sections.

First, it means that the four-letter substructure  $\{a, b, c, d\}$  introduced in section 5 is a *second-order alphabet* — a set of recurring patterns of length 6 over the binary tape. The higher symbolic structure of the prime distribution emerges from a binary foundation, in the same way that complex behavior emerges from  $\{0, 1\}$  in cellular automata theory [24].

Second, it makes the connection to  $S$ -adic theory precise. The substitution morphisms defined in Section 5 act on binary words, which places the automaton squarely within the framework of Fogg [12] and Berthé and Delecroix [4], where the foundational results are stated for substitutions over finite — often binary — alphabets.

**3.6. Illustrative Example: First Five Steps.** The first five states of the automaton are shown in Table 1.

$n$	$E_n$	$CP_n$	Width
1	ONE	$\langle L \rangle$	1
2	$P$	$\langle LM \rangle$	2
3	$P$	$\langle MLMLMM \rangle$	6
4	$M$	$\langle LMLMMM \rangle$	6
5	$P$	$\langle MLMMM LMLMMM LMLMMM LMMMMM LMLMMM M \rangle$	30

TABLE 1. First five states of the automaton. At step  $n = 2$ , the tape expands from width 1 to width 2 and the filter marks position 2 as  $M$ . At step  $n = 3$ , the tape expands from width 2 to width 6 and the filter marks positions 3 and 6 as  $M$ . At step  $n = 4$ ,  $E_4 = M$  because  $CP_3[1] = M$  — the number 4 is composite — and only the shift is applied. At step  $n = 5$ , the tape expands from width 6 to width 30 and the filter marks all multiples of 5.

The binary nature of the tape is visible throughout: every cell carries exactly one of two symbols, and the growing complexity of the pattern arises entirely from the interaction of the three operators over successive steps.

The algorithm is displayed in a more visually accessible way in Figure 5 with the first four steps. It is shown how at step 1 the  $L$  covers the whole number ray, thus is a periodic  $\langle L \rangle$  and how this  $\langle L \rangle$  transforms into the periodic  $\langle LM \rangle$  and so on.

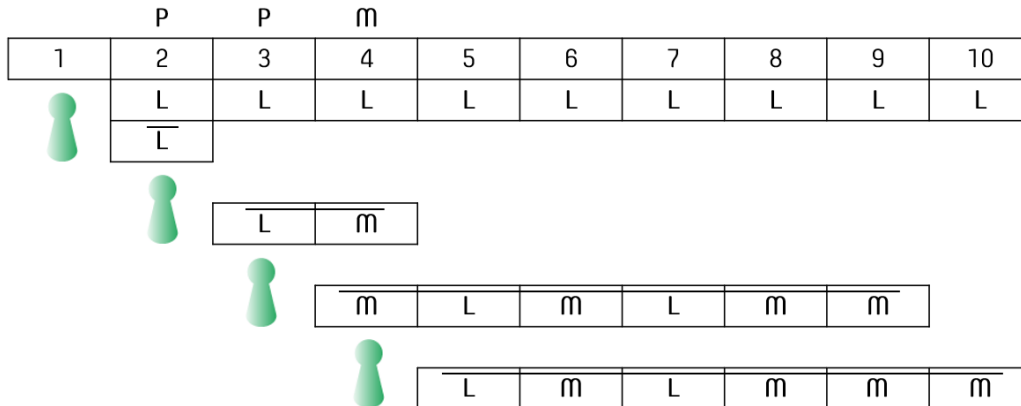


FIGURE 5. The algorithm: The green playing piece marks the current position of the reading head — the natural number  $n$  being processed at each step. As the reading head advances from  $n = 1$  to  $n = 4$ , the tape  $CP_n$  grows: at  $n = 2$  the tape has width 2, at  $n = 3$  width 6, at  $n = 4$  width 6 with a shift.

#### 4. SYNCHRONIZATION AND EQUIVALENCE TO THE SIEVE OF ERATOSTHENES

**4.1. Synchronization.** The automaton processes one natural number per step. The following lemma establishes that the symbol at position  $CP_n[1]$  always corresponds to the natural number  $n$ , so that the encoding function  $\mu_n$  reads the correct symbol at every step.

**Lemma 1** (Synchronization). *For every step  $n \geq 1$ , the symbol at position  $CP_{n-1}[1]$  corresponds to the natural number  $n$ .*

*Proof.* We proceed by induction on  $n$ .

*Base case.* At step  $n = 1$ , the tape consists of a single cell  $CP_1 = \langle L \rangle$ , and Register  $N$  holds  $N_1 = 1$ . The symbol  $CP_1[1] = L$  corresponds to the number 1 by initialization.

*Inductive step.* Assume that at step  $n$ , the symbol at position  $CP_{n-1}[1]$  corresponds to the natural number  $n$ . We show that after the transition at step  $n$ , the symbol at position  $CP_n[1]$  corresponds to  $n + 1$ .

There are two cases.

If  $E_n = M$ , then  $CP_n = S_n(CP_{n-1})$ . The shift operator removes  $CP_{n-1}[1]$  from the left and appends it to the right. The new first cell  $CP_n[1]$  is therefore the cell that was previously at position  $CP_{n-1}[2]$ , which by the inductive hypothesis corresponds to the natural number  $n + 1$ .

If  $E_n = P$ , then  $CP_n = F_n(X_n(S_n(CP_{n-1})))$ . The shift is applied first, giving the same alignment as in the composite case. The expansion  $X_n$  then replicates the tape  $n$  times — but since  $X_n$  appends copies to the right, the leftmost cell  $CP[1]$  is unchanged by the expansion. The filter  $F_n$  traverses the tape with step size  $n$  beginning at position  $n$ , so it does not affect position 1. Therefore  $CP_n[1]$  after the full transition is the same cell that became  $CP[1]$  after the shift, which corresponds to  $n + 1$ .

In both cases,  $CP_n[1]$  corresponds to  $n + 1$  after the transition at step  $n$ . By induction, the synchronization holds for all  $n \geq 1$ .  $\square$

*Remark 1.* The synchronization lemma is what makes the encoding function  $\mu_n$  well-defined. Without it, the symbol read by Register  $E$  at step  $n$  would not necessarily correspond to the number  $n$ , and the automaton would not correctly classify primes and composites.

**4.2. Equivalence to the Sieve of Eratosthenes.** We now prove the central equivalence result. The Sieve of Eratosthenes classifies every integer  $n \geq 2$  as prime if and only if  $n$  has no prime divisor  $p < n$ . The following theorem shows that the automaton produces exactly the same classification.

**Theorem 1** (Equivalence to the Sieve of Eratosthenes). *For every integer  $n \geq 2$ :*

$$(7) \quad n \in \mathbb{P} \iff \text{CP}_{n-1}[1] = L$$

$$(8) \quad n \notin \mathbb{P} \iff \text{CP}_{n-1}[1] = M$$

*Therefore, the automaton produces exactly the same classification of every natural number as the Sieve of Eratosthenes.*

*Proof.* By Lemma 1, the symbol at position  $\text{CP}_{n-1}[1]$  corresponds to the natural number  $n$  at step  $n$ .

( $\Rightarrow$ ) *Suppose  $n$  is prime.* Then  $n$  has no prime divisor  $p$  with  $2 \leq p < n$ . For every prime  $p < n$ , the filter operator  $F_p$  is applied at step  $p$  with step size  $p$ , marking every  $p$ -th position as  $M$ . Since  $p \nmid n$ , the position corresponding to  $n$  is not visited by  $F_p$ . This holds for every prime  $p < n$ . Therefore no filter operator applied before step  $n$  affects the position corresponding to  $n$ , and its symbol remains  $L$  from initialization. Hence  $\text{CP}_{n-1}[1] = L$ .

( $\Leftarrow$ ) *Suppose  $n$  is composite.* Then there exists at least one prime  $p$  with  $2 \leq p < n$  such that  $p \mid n$ . At step  $p$ , the filter operator  $F_p$  is applied with step size  $p$ . Since  $n$  is a multiple of  $p$ , the position corresponding to  $n$  is visited by  $F_p$ , and its symbol is changed from  $L$  to  $M$ . Since  $p < n$ , this occurs strictly before step  $n$ . Therefore  $\text{CP}_{n-1}[1] = M$ .

The two directions together establish the biconditional for both primality and compositeness. The automaton produces exactly the same classification of every integer  $n \geq 2$  as the Sieve of Eratosthenes.  $\square$

*Remark 2* (The number 1). The number 1 is processed at step  $n = 1$  with encoding  $E_1 = \text{ONE}$ . It is neither prime nor composite and is excluded from Theorem 1. The symbol ONE in Register  $E$  ensures that no filter operator is triggered at step 1, and the tape evolves from  $\text{CP}_1 = \langle L \rangle$  to  $\text{CP}_2 = \langle LM \rangle$  at the next prime step without interference.

**4.3. Width of the Tape.** The following lemma establishes the growth rate of the tape, which will be needed in subsequent sections.

**Lemma 2** (Width of the tape). *For every step  $n \geq 1$ :*

$$(9) \quad |\text{CP}_n| = \prod_{p \leq n} p$$

*where the product runs over all primes  $p \leq n$ . For  $n = 1$ , the empty product equals 1 by convention.*

*Proof.* At step  $n = 1$ , the tape has exactly one cell, so  $|\text{CP}_1| = 1$ , consistent with the empty product.

For  $n > 1$ , we consider two cases.

If  $n$  is composite, then  $CP_n = S_n(CP_{n-1})$ . The shift does not change the width, so  $|CP_n| = |CP_{n-1}|$ . The set of primes  $p \leq n$  equals the set of primes  $p \leq n-1$ , so the product is unchanged.

If  $n$  is prime, then  $CP_n = F_n(X_n(S_n(CP_{n-1})))$ . The shift does not change the width. The expansion  $X_n$  replicates the tape  $n$  times, so  $|X_n(S_n(CP_{n-1}))| = n \cdot |CP_{n-1}|$ . The filter  $F_n$  does not change the width. Therefore  $|CP_n| = n \cdot |CP_{n-1}|$ .

Since the width increases by a factor of  $p$  at every prime step  $p$  and is unchanged at composite steps, it follows by induction that  $|CP_n| = \prod_{p \leq n} p$ .  $\square$

*Remark 3* (Computational complexity). The width of the tape grows as the primorial  $\prod_{p \leq n} p$ , which increases superexponentially. By the Prime Number Theorem,  $\ln(\prod_{p \leq n} p) \sim n$ , so the primorial grows roughly as  $e^n$ . This superexponential growth confirms that the automaton is not intended as a computationally efficient method for generating primes. Its purpose is structural and analytical, as established in Section 1. The Frozen Window technique introduced in Section 8 circumvents this limitation for experimental purposes.

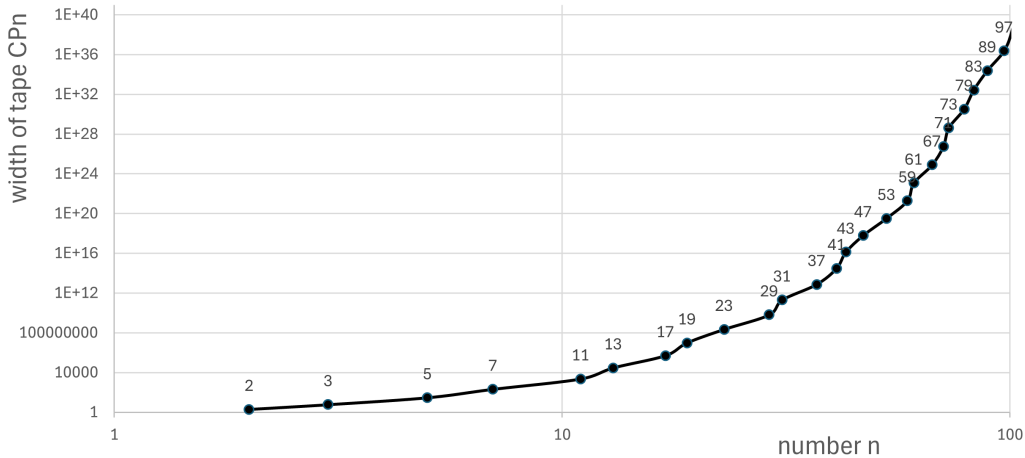


FIGURE 6. Width of the tape  $CP_n$  as a function of  $n$  (logarithmic scale). The width equals the primorial  $\prod_{p \leq n} p$  and grows superexponentially — faster than any exponential function. This growth is not an artifact of the representation: by Lemma 2, it is a structural consequence of the expansion operator  $X_n$  and cannot be compressed without destroying the periodic symbolic structure of the tape. At  $n = 97$  the tape width already exceeds  $10^{36}$ .

## 5. THE FOUR-LETTER SUBSTRUCTURE

**5.1. Emergence of the Substructure.** After the expansion and filtering steps at  $n = 2$  and  $n = 3$ , the tape at step  $n = 4$  has width 6 and carries the binary word:

$$(10) \quad CP_4 = \langle L M L M M M \rangle$$

This word is the fundamental building block of all subsequent tape states. We will show that for every step  $n \geq 4$ , the tape  $\text{CP}_n$  consists entirely of concatenated copies of four recurring blocks of width 6 over the binary alphabet  $\Sigma_{\text{CP}} = \{L, M\}$ . These four blocks define a second-order alphabet that captures the complete symbolic structure of the prime candidate distribution.

**Definition 1** (Four-letter alphabet). The four letters are defined as binary words of length 6 over  $\Sigma_{\text{CP}} = \{L, M\}$ :

$$(11) \quad a := \langle L M L M M M \rangle$$

$$(12) \quad b := \langle L M M M M M \rangle$$

$$(13) \quad c := \langle M M L M M M \rangle$$

$$(14) \quad d := \langle M M M M M M \rangle$$

The second-order alphabet is  $\Sigma_2 = \{a, b, c, d\}$ .

*Remark 4* (Recursive Base Patterns and the Emergent Letter  $e$ ). The four-letter alphabet  $\Sigma_2 = \{a, b, c, d\}$  is not a static endpoint but the first stage of a recursive hierarchy. At every prime step  $p$ , the entire periodic tape  $\text{CP}_{p-1}$  serves as a new *base pattern* (a higher-order meta-letter). For example, the tape  $\text{CP}_4 = \langle a \rangle$  serves as the base pattern for the next level of complexity; under the transition for the prime  $p = 5$ , this single block of  $a$  is expanded and filtered to become the meta-letter  $e = aabac$ . The symbolic evolution of the sieve is thus a sequence of alphabet renormalizations, where the cumulative output (the tape) of one prime step becomes the fundamental "single letter" to be varied by the next.

**5.2. Structural Interpretation.** The four letters carry distinct arithmetic meaning that makes them natural objects of analysis.

**Letter  $a = \langle LMLMMM \rangle$**  carries two  $L$  symbols at positions 1 and 3 within the block. These two positions are separated by exactly one  $M$ , corresponding to a gap of 2 in the number line. Letter  $a$  is therefore the *twin prime template*: whenever  $a$  survives all filtering steps and its two  $L$  symbols reach Register  $E$ , they encode a pair of numbers differing by 2, both prime candidates. Letter  $a$  is the only element of  $\Sigma_2$  that can produce twin primes.

**Letter  $b = \langle LMMMMM \rangle$**  carries one  $L$  symbol at position 1 and five  $M$  symbols. It is a single prime candidate with no twin. It arises when the left  $L$  of a twin prime template is eliminated by a filter.

**Letter  $c = \langle MMLMMM \rangle$**  carries one  $L$  symbol at position 3 and five  $M$  symbols. It is also a single prime candidate with no twin. It arises when the right  $L$  of a twin prime template is eliminated by a filter.

**Letter  $d = \langle MMMMMM \rangle$**  carries no  $L$  symbols. It is a block of six consecutive composites — a prime gap of width at least 6. Clusters of letter  $d$  correspond to arbitrarily large prime gaps.

*Remark 5* (Completeness). The four letters  $a, b, c, d$  are the only binary words of length 6 that appear in  $\text{CP}_n$  for any  $n \geq 4$ . Of the  $2^6 = 64$  possible binary words of length 6 over  $\Sigma_{\text{CP}} = \{L, M\}$ , only four appear. This is a structural consequence of the dynamics: the four letters are precisely the reachable states of a block of width 6 under the action of the filter operator, starting from the initial block  $a = \langle LMLMMM \rangle$  at step  $n = 4$ . Since the filter

acts with step size  $n \geq 5$  for all prime steps after  $n = 3$ , which exceeds the distance of 2 between the two  $L$  symbols in letter  $a$ , at most one  $L$  per block can be eliminated at each prime step Figure 7. The set  $\{a, b, c, d\}$  is therefore closed under the transition rules — no new block types can be created — and exhaustive over all states reachable from the initial configuration.

### 5.3. Stability of the Substructure.

**Lemma 3** (Stability of  $\Sigma_2$ ). *For every step  $n \geq 4$ , the tape  $CP_n$  consists entirely of concatenated blocks from  $\Sigma_2 = \{a, b, c, d\}$ .*

*Proof.* At step  $n = 4$ ,  $CP_4 = \langle LMLMMM \rangle = \langle a \rangle$ , which is a single block of letter  $a$ . The claim holds at the base case.

For the inductive step, assume that  $CP_{n-1}$  consists entirely of blocks from  $\Sigma_2$ . We consider the two cases of the transition function.

If  $E_n = M$ , then  $CP_n = S_n(CP_{n-1})$ . The shift moves one symbol from the left end to the right end. Since the tape is strictly periodic and the period length is a multiple of 6 for all  $n \geq 4$  by Lemma 2, the shift preserves the block decomposition — the rotated tape still consists entirely of blocks from  $\Sigma_2$ .

If  $E_n = P$ , then  $CP_n = F_n(X_n(S_n(CP_{n-1})))$ . The shift preserves the block decomposition as above. The expansion  $X_n$  replicates the tape  $n$  times — since each copy consists entirely of blocks from  $\Sigma_2$ , the expanded tape also consists entirely of blocks from  $\Sigma_2$ . The filter  $F_n$  acts with step size  $n \geq 5$ , replacing  $L$  symbols with  $M$  at every  $n$ -th position. Since the step size  $n$  exceeds the distance of 2 between the two  $L$  symbols within any block of letter  $a$ , a single stride of  $F_n$  can change at most one  $L$  within any given block. The only possible symbol change within a block is  $L \rightarrow M$ , which transforms blocks as follows:

- $a \rightarrow b$  (left  $L$  eliminated)
- $a \rightarrow c$  (right  $L$  eliminated)
- $b \rightarrow d$  (single  $L$  eliminated)
- $c \rightarrow d$  (single  $L$  eliminated)
- $d \rightarrow d$  (no  $L$  present, unchanged)

In every case the result is again a block from  $\Sigma_2$ . Therefore  $CP_n$  consists entirely of blocks from  $\Sigma_2$  after the full transition. By induction the claim holds for all  $n \geq 4$ .  $\square$

**5.4. Transition Rules.** The proof of Lemma 3 implicitly defines the transition rules of the second-order alphabet. We make them explicit here.

At each prime step  $n \geq 5$ , the filter operator  $F_n$  can transform letters as follows:

- $a \rightarrow b$  (left  $L$  of twin template eliminated)
- $a \rightarrow c$  (right  $L$  of twin template eliminated)
- $a \rightarrow a$  (neither  $L$  eliminated)
- $b \rightarrow d$  (single  $L$  eliminated)
- $b \rightarrow b$  ( $L$  not visited by filter)
- $c \rightarrow d$  (single  $L$  eliminated)
- $c \rightarrow c$  ( $L$  not visited by filter)
- $d \rightarrow d$  (no  $L$  present — unchanged)

Three observations follow directly from these rules.

First, the transitions are irreversible over the binary tape: once an  $L$  is changed to  $M$ , it cannot be restored. The sequence  $a \rightarrow \{b, c\} \rightarrow d$  is a one-way path.

Second, letter  $d$  is an absorbing state in the transition graph. Once a block reaches  $d$ , it remains  $d$  at all subsequent steps.

Third, and most importantly: *letter  $a$  can only be destroyed, never created, by the filter operator.* New copies of letter  $a$  can only appear through the expansion operator  $X_n$ , which replicates existing blocks. This asymmetry between creation (by expansion) and destruction (by filtering) is the structural foundation of the Hydra Effect developed in Section 5.

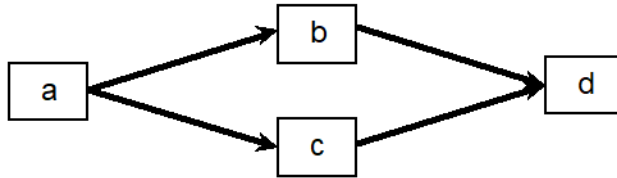


FIGURE 7. Transition rules of the four letters  $\Sigma_2 = \{a, b, c, d\}$ . Letter  $a$  (twin prime template  $\langle LMLMMM \rangle$ ) can transition to either  $b$  or  $c$  when one of its two  $L$  symbols is eliminated by a filter operator. Letters  $b$  and  $c$  (single prime candidates) transition to  $d$  when their remaining  $L$  symbol is eliminated. Letter  $d$  (six consecutive composites) is an absorbing state. All transitions are irreversible over the binary tape alphabet  $\Sigma_{CP} = \{L, M\}$ .

**5.5. Lemma on Three Consecutive Primes.** The four-letter structure allows us to prove a simple but precise result about prime triples.

**Lemma 4** (No three consecutive odd primes beyond 3, 5, 7). *For  $n \geq 4$ , pattern  $\langle LMLML \rangle$  — corresponding to three numbers in arithmetic progression with common difference 2, all prime candidates — does not appear in  $CP_n$ .*

*Proof.* The pattern  $\langle LMLML \rangle$  has length 5 and would require two consecutive blocks from  $\Sigma_2$  whose combined first five symbols are  $LMLML$ . Examining all sixteen possible concatenations of two blocks from  $\{a, b, c, d\}$ , no pair produces this pattern at the block boundary or

within a block of width 6. The only block carrying two  $L$  symbols is letter  $a = \langle LMLMMM \rangle$ , whose fifth symbol is  $M$ , not  $L$ . Therefore  $\langle LMLML \rangle$  cannot appear in any tape  $CP_n$  for  $n \geq 4$ .  $\square$

*Remark 6.* This result is consistent with the known fact that the only prime triple of the form  $(p, p + 2, p + 4)$  is  $(3, 5, 7)$ , since for any larger  $p$  one of  $p, p + 2, p + 4$  is divisible by 3. Lemma 4 provides a structural, symbolic proof of this constraint within the automaton framework.

## 6. SUBSTITUTION MORPHISMS, TRANSITION MATRIX, AND THE HYDRA EFFECT

**6.1. Substitution Morphisms.** The transition rules established in Section 4.4 define a family of substitution morphisms over the second-order alphabet  $\Sigma_2 = \{a, b, c, d\}$ . At each prime step  $n$  with prime  $p_n$ , the filter operator  $F_{p_n}$  acts on the tape by transforming blocks according to the reachable transitions. We formalize this as a morphism  $\sigma_{p_n} : \Sigma_2^* \rightarrow \Sigma_2^*$ .

The morphisms are defined as follows. At prime step  $p$ , each letter is mapped to a word over  $\Sigma_2$  that reflects the combined effect of expansion and filtering:

$$(15) \quad \sigma_p(a) = a^{p-2} b c$$

$$(16) \quad \sigma_p(b) = b^{p-1} d$$

$$(17) \quad \sigma_p(c) = c^{p-1} d$$

$$(18) \quad \sigma_p(d) = d^p$$

where the exponent denotes concatenation —  $a^{p-2}$  means  $p - 2$  consecutive copies of letter  $a$ .

**Derivation of equation (15).** At prime step  $p$ , the expansion operator  $X_p$  replicates the tape  $p$  times. A single block of letter  $a$  therefore produces  $p$  copies. Of these  $p$  copies, the filter  $F_p$  eliminates exactly one  $L$  from exactly two copies — the left  $L$  of one copy (producing letter  $b$ ) and the right  $L$  of another copy (producing letter  $c$ ). The remaining  $p - 2$  copies are not visited by the filter at their  $L$  positions and survive as letter  $a$ . This gives  $\sigma_p(a) = a^{p-2} b c$ .

**Derivation of equation (16).** Letter  $b$  carries one  $L$  symbol. After expansion,  $p$  copies of  $b$  are produced — both pre-existing  $b$  blocks and  $b$  blocks newly created from destroyed  $a$  blocks at this step. The filter  $F_p$  acts on the fully expanded tape with step size  $p$ . By the Chinese Remainder Theorem, exactly one copy of each  $b$  block is visited at its  $L$  position and converted to  $d$ . The remaining  $p - 1$  copies survive as  $b$ . Newly created  $b$  blocks from destroyed  $a$  blocks are not visited again by the filter at the same step, because their position was already the target of the stride that destroyed the parent  $a$  block. This gives  $\sigma_p(b) = b^{p-1} d$ .

**Derivation of equation (17).** By the same argument as equation (16), since letter  $c$  also carries exactly one  $L$  symbol and newly created  $c$  blocks from destroyed  $a$  blocks are similarly not revisited by the filter. This gives  $\sigma_p(c) = c^{p-1} d$ .

**Derivation of equation (18).** Letter  $d$  carries no  $L$  symbols. The filter has no effect on any copy. After expansion, all  $p$  copies remain as  $d$ . This gives  $\sigma_p(d) = d^p$ .

*Remark 7 (Chinese Remainder Theorem).* The claim that the filter visits exactly one copy of each  $L$ -bearing letter at its  $L$  position follows from the Chinese Remainder Theorem. Since  $p$  is a new prime at step  $p$ , it is coprime to the previous tape width  $w = p_{n-1}\#$ . The congruence  $x + k \cdot w \equiv 0 \pmod{p}$  has exactly one solution for  $k$  in the range  $[0, p - 1]$ . Therefore each

$L$  position in the tape is visited by the filter exactly once across the  $p$  copies produced by expansion. This guarantees the precise counts in equations (15)–(18).

*Remark 8* (Consistency of morphisms under composition). The morphisms  $\sigma_p$  are applied to the tape as it exists after expansion — that is, to all  $p$  copies of all blocks simultaneously, including blocks newly created by the transformation of letter  $a$ . The filter  $F_p$  acts exactly once on this expanded tape and visits each  $L$  position at most once. Therefore the morphisms  $\sigma_p(a)$ ,  $\sigma_p(b)$ ,  $\sigma_p(c)$ ,  $\sigma_p(d)$  describe the net effect of the full transition on each block type, and they are mutually consistent: the output of  $\sigma_p(a)$  feeds into the population of  $b$  and  $c$ , but those newly created blocks are not filtered again within the same step.

**6.2. Transition Matrix.** The substitution morphisms of the previous subsection are encoded in a prime-dependent transition matrix  $M_p$ . The entry  $M_p[i, j]$  gives the number of times letter  $j$  appears in  $\sigma_p(i)$ , where the ordering of letters is  $(a, b, c, d)$ .

**Definition 2** (Transition matrix).

$$(19) \quad M_p = \begin{pmatrix} p-2 & 1 & 1 & 0 \\ 0 & p-1 & 0 & 1 \\ 0 & 0 & p-1 & 1 \\ 0 & 0 & 0 & p \end{pmatrix}$$

This matrix has three immediately visible properties.

First, it is *upper triangular*. All entries below the main diagonal are zero. This reflects the irreversibility of the transitions established in Section 4.4: letters can only move toward  $d$ , never back toward  $a$ .

Second, the *eigenvalues are the diagonal entries*:  $p-2$ ,  $p-1$ ,  $p-1$ , and  $p$ . They are read directly from the matrix without computation. The eigenvalue  $p-2$  governs the growth of letter  $a$  — the twin prime template. The eigenvalue  $p-1$  governs letters  $b$  and  $c$ . The eigenvalue  $p$  governs letter  $d$ , reflecting the fact that composites accumulate at the fastest rate.

Third, the *symmetry between  $b$  and  $c$*  is visible in the identical rows 2 and 3. The system treats the left-survivor and right-survivor of a destroyed twin prime template identically. There is no asymmetry between the two sides.

**Population vector.** Let  $\mathbf{v}_n = (|a|, |b|, |c|, |d|)$  denote the population vector at prime step  $n$ , where each entry counts the number of occurrences of the corresponding letter in  $\text{CP}_n$ . The population at the next prime step  $n'$  is obtained by:

$$(20) \quad \mathbf{v}_{n'} = \mathbf{v}_n \cdot M_p$$

**6.3. The Hydra Effect.** The morphism  $\sigma_p(a) = a^{p-2}bc$  describes a growth-and-elimination dynamic that we term the *Hydra Effect*, by analogy with the mythological creature that grows new heads faster than they can be removed. At each prime step  $p$ , every existing copy of letter  $a$  first multiplies into  $p$  copies through expansion, and then two of those copies are converted to  $b$  and  $c$  by the filter. The net survival rate per copy is  $p-2$  out of  $p$ .

**Definition 3** (Hydra Equation). Let  $G_n(a) = |a_n|$  denote the count of letter  $a$  at prime step  $n$ , and let  $p_n$  denote the  $n$ -th prime. Then:

$$(21) \quad G_n(a) = G_{n-1}(a) \cdot (p_n - 2)$$

*Proof.* At prime step  $p_n$ , the expansion operator produces  $p_n$  copies of every existing block. Of the  $p_n$  copies of each letter  $a$  block, exactly two are converted by the filter — one to  $b$  and one to  $c$  — and  $p_n - 2$  survive as  $a$ . Since this holds independently for every existing copy of letter  $a$ , the total count after the step is  $G_{n-1}(a) \cdot (p_n - 2)$ .  $\square$

**Corollary 1** (Geometric growth of twin prime templates). *Starting from  $G_4(a) = 1$  at step  $n = 4$ , the count of letter  $a$  at prime step  $p_n$  satisfies:*

$$(22) \quad G_n(a) = \prod_{\substack{p_k \leq p_n \\ p_k \geq 5}} (p_k - 2)$$

The first several values are shown in Table 2.

$n$	Growth	Elimination	$G_n(a)$	Automaton count
4	—	—	1	1
5	5	2	3	3
7	21	6	15	15
11	165	30	135	135
13	1755	270	1485	1485
17	25245	2970	22275	22275

TABLE 2. Hydra calculation versus direct automaton count of letter  $a$ . The agreement between the analytical formula and the automaton count is exact at every step verified.

#### 6.4. Connection to OEIS A059861 and Hardy–Littlewood.

**Lemma 5** (Connection to OEIS A059861). *The sequence  $G_n(a)$  defined by the Hydra Equation (21) is identical to OEIS sequence A059861, which counts the number of differences of size 2 in a reduced residue system modulo  $p_n\#$ .*

*Proof.* The reduced residue system modulo  $p_n\#$  consists of all integers in  $[1, p_n\#]$  coprime to  $p_n\#$ . A difference of size 2 in this system corresponds to a pair  $(k, k + 2)$  both coprime to  $p_n\#$ . The count of such pairs is exactly the number of twin prime templates — positions where both  $k$  and  $k + 2$  survive all filters  $F_p$  for  $p \leq p_n$ . This is precisely what the automaton counts as letter  $a$  in  $CP_n$ . The Hydra Equation gives the same recurrence as the formula for A059861, and the initial value  $G_4(a) = 1$  matches. Therefore the sequences are identical.  $\square$

*Remark 9* (Hardy–Littlewood connection). The density of twin prime templates at prime step  $p_n$  is given by the relative count of letter  $a$  normalized by the tape width:

$$(23) \quad \text{Density}(a)_n = \frac{G_n(a)}{p_n\#} \propto \prod_{\substack{p_k \geq 3 \\ p_k \leq p_n}} \left(1 - \frac{2}{p_k}\right)$$

This product is precisely the singular series factor  $C_2$  appearing in the Hardy–Littlewood twin prime conjecture [15], which predicts that the number of twin prime pairs up to  $x$  grows

as:

$$(24) \quad \pi_2(x) \sim 2C_2 \cdot \frac{x}{(\ln x)^2}$$

The automaton does not prove the Hardy–Littlewood conjecture. What it provides is a deterministic, constructive derivation of the combinatorial factor  $C_2$  as a structural property of the transition matrix  $M_p$  — specifically, as the product of the normalized eigenvalues  $(p - 2)/p$  for the letter  $a$  row. This is not a probabilistic heuristic but a consequence of the Chinese Remainder Theorem applied to the filter operator.

**6.5. Normalized Transition Matrix and Asymptotic Densities.** Dividing  $M_p$  by the growth factor  $p$  yields the normalized transition matrix  $W_p$ , which describes the relative survival rates of each letter as the tape expands:

$$(25) \quad W_p = \frac{1}{p} \cdot M_p = \begin{pmatrix} \frac{p-2}{p} & \frac{1}{p} & \frac{1}{p} & 0 \\ 0 & \frac{p-1}{p} & 0 & \frac{1}{p} \\ 0 & 0 & \frac{p-1}{p} & \frac{1}{p} \\ 0 & 0 & 0 & 1 \end{pmatrix}$$

The asymptotic behavior of the densities follows directly from the normalized eigenvalues:

- The density of letter  $d$  converges to 1. Almost all positions become composite as  $n \rightarrow \infty$ , consistent with the Prime Number Theorem.
- The densities of letters  $b$  and  $c$  decay at rate  $(p - 1)/p$  per prime step and converge to 0.
- The density of letter  $a$  decays at rate  $(p - 2)/p$  per prime step — twice as fast as  $b$  and  $c$  — and also converges to 0.

However, the decay of letter  $a$  is slow. The product  $\prod_{p \geq 3} (1 - 2/p)$  diverges to 0 only because the sum  $\sum 2/p$  diverges — a consequence of Mertens’ theorem [20]. The density of twin prime templates therefore approaches 0, but does so arbitrarily slowly. While letter  $a$  becomes rare, it is never structurally eliminated — new copies are always created by the expansion operator before the filter can act. This is the formal content of the Hydra Effect: the template persists structurally even as its density vanishes.

**6.6. Hierarchical Renormalization: The Emergent Letter  $e$ .** The transition matrix  $M_p$  describes the relative populations of the second-order blocks, but the spatial arrangement of these blocks follows a recursive, hierarchical logic. At step  $n = 4$ , the tape  $CP_4$  consists of a single block of letter  $a = \langle LMLMMM \rangle$ , which serves as the *base pattern* for the next prime step.

Under the transition for the prime  $p = 5$ , this base pattern  $a$  undergoes expansion and filtering to produce a third-order meta-letter  $e \in \Sigma_3$ . Specifically, the expansion operator  $X_5$  replicates the base pattern into five identical copies ( $a^5$ ), and the filter operator  $F_5$  then eliminates precisely two  $L$  symbols across these copies (one at position 15 and one at position 25). The resulting variation of the base pattern defines the meta-letter  $e$ :

$$(26) \quad e := a a b a c$$

This indicates that the Sieve of Eratosthenes is a constructive evolution of base patterns. Each prime  $p_{\text{next}}$  takes the tape  $\text{CP}_{p_{\text{prev}}}$  as a stable foundation and generates a new, longer meta-letter that serves as the basis for the subsequent prime's variation. The symbolic complexity of the number line thus grows through a sequence of such nested hierarchical renormalizations.

## 7. THE STABILITY ZONE

**7.1. Definition and Motivation.** The automaton processes natural numbers sequentially, one per step. At step  $n$ , the filter operator  $F_n$  acts with step size  $n$ , marking every  $n$ -th position on the tape as composite. The first position visited by  $F_n$  is position  $n$  itself — the first multiple of  $n$  within the tape. This means that all positions between the current head of the tape and position  $n$  are not touched by  $F_n$  at step  $n$ .

This observation has a cumulative consequence. For any position corresponding to a number  $m$  in the interval  $(n, 2n)$ , the following holds: the smallest prime that could mark  $m$  as composite is a prime  $p$  with  $p \mid m$  and  $p < m$ . But since  $m > n$ , any such prime  $p$  satisfies  $p \leq m/2 < n$  — meaning  $F_p$  was applied at a step strictly before step  $n$ . All future filter operators  $F_q$  with  $q > n$  have step size  $q > n$  and therefore cannot reach position  $m$  within the interval  $(n, 2n)$  before step  $m$  itself.

This defines a zone of immutability that advances with the automaton.

**Definition 4** (Stability Zone). At step  $n$ , the Stability Zone is the interval:

$$(27) \quad \text{SZ}_n = [n + 1, 2n - 1]$$

All positions within  $\text{SZ}_n$  that carry the symbol  $L$  at step  $n$  are *stable survivors* — they will not be marked as composite by any filter operator applied between step  $n$  and the step at which they reach Register  $E$ .

## 7.2. Proof of Immutability.

**Theorem 2** (Stability Zone). *For every step  $n \geq 2$  and every position  $m \in [n + 1, 2n - 1]$ , if  $\text{CP}_n[m] = L$  then  $\text{CP}_{m-1}[1] = L$ . That is, no filter operator applied between step  $n$  and step  $m - 1$  changes the symbol at position  $m$  from  $L$  to  $M$ .*

*Proof.* Let  $m \in [n + 1, 2n - 1]$  and suppose  $\text{CP}_n[m] = L$ . We must show that no filter operator  $F_q$  with  $n < q < m$  changes the symbol at position  $m$ .

A filter operator  $F_q$  changes the symbol at position  $m$  from  $L$  to  $M$  if and only if  $q \mid m$ , that is, if  $m$  is a multiple of  $q$ . We show that no such  $q$  exists in the range  $(n, m)$ .

Suppose for contradiction that there exists a prime  $q$  with  $n < q < m$  and  $q \mid m$ . Then  $m \geq 2q > 2n$ , which contradicts  $m \leq 2n - 1$ . Therefore no prime  $q$  in the range  $(n, m)$  divides  $m$ .

Since filter operators are only applied at prime steps, and no prime  $q$  in  $(n, m)$  divides  $m$ , no filter operator applied strictly between step  $n$  and step  $m$  can affect position  $m$ . The symbol at position  $m$  remains  $L$  from step  $n$  until step  $m - 1$ , at which point  $\text{CP}_{m-1}[1] = L$  by the synchronization of Lemma 1.  $\square$

*Remark 10* (Bertrand's Postulate). The Stability Zone is non-empty for all  $n \geq 2$  — that is, the interval  $[n + 1, 2n - 1]$  always contains at least one integer. More importantly, by

Bertrand's Postulate [6, 23, 11], for every  $n \geq 2$  there exists at least one prime  $p$  with  $n < p < 2n$ . Therefore the Stability Zone always contains at least one prime, and the automaton always produces at least one new confirmed prime per pass through the Stability Zone. This is consistent with the infinitude of primes.

Recent results strengthen this guarantee considerably. Nagura [21] showed that a prime always exists in  $(n, 6n/5)$  for  $n \geq 25$ , and Axler [3] established an explicit prime in  $(x, x(1 + 198.2/\log^4 x))$  for  $x > 1$ . For almost all  $n$ , Li [17] shows that the much shorter interval  $[n, n + n^{1/21.5+\varepsilon}]$  contains a prime. These results imply that the Stability Zone is not merely non-empty — it is richly populated with confirmed prime candidates for all sufficiently large  $n$ .

*Remark 11* (Dynamical interpretation of Bertrand's interval). The boundaries of the Stability Zone coincide exactly with the interval of Bertrand's Postulate. This is not a design choice but a structural consequence of the filter operator acting with step size  $n$ : the first stride of  $F_n$  lands at position  $n$ , leaving  $[n + 1, 2n - 1]$  untouched. The Stability Zone thus provides a dynamical systems interpretation of Bertrand's interval.

**7.3. Advancement of the Stability Zone.** The Stability Zone advances as  $n$  increases. At each step, the interval  $[n + 1, 2n - 1]$  shifts by one position to the right and simultaneously expands.

**Lemma 6** (Advancement). *From step  $n$  to step  $n + 1$ , the left boundary of the Stability Zone advances by one position and the right boundary advances by two positions:*

$$(28) \quad \text{SZ}_n = [n + 1, 2n - 1] \longrightarrow \text{SZ}_{n+1} = [n + 2, 2n + 1]$$

*The width of  $\text{SZ}_n$  is  $n - 1$  and increases by one at each step.*

*Proof.*  $|\text{SZ}_n| = 2n - 1 - (n + 1) + 1 = n - 1$ .

$|\text{SZ}_{n+1}| = 2n + 1 - (n + 2) + 1 = n$ .

The left boundary advances by one. The right boundary advances by two. The width increases by one at each step.  $\square$

*Remark 12* (Why advancement by two matters). The right boundary advances by two positions at each step. This means that at every step, two new positions enter the Stability Zone from the right. Without this advancement by two, no new prime candidates could enter the Stability Zone after  $n = 2$ , and the automaton would cease to produce primes beyond 2. The advancement by two is therefore not a technical detail but a structural necessity.

**7.4. Confirmed Primes in the Stability Zone.**

**Corollary 2** (Primes in the Stability Zone). *For every  $n \geq 2$ , the set of primes in the interval  $[n + 1, 2n - 1]$  is in exact correspondence with the  $L$  symbols in  $\text{SZ}_n$ .*

*Proof.* By Theorem 2, every  $L$  in  $\text{SZ}_n$  survives until its position reaches Register  $E$ , at which point it is encoded as  $P$ . By Theorem 1, a number is encoded as  $P$  if and only if it is prime. Therefore the  $L$  symbols in  $\text{SZ}_n$  correspond exactly to the primes in  $[n + 1, 2n - 1]$ .  $\square$

**7.5. Visual Representation.** The advancement of the Stability Zone is shown in Table 3, with stable  $L$  survivors marked for the first eleven steps.

Step $n$	$SZ_n = [n + 1, 2n - 1]$	Confirmed primes in $SZ_n$
2	[3, 3]	3
3	[4, 5]	5
4	[5, 7]	5, 7
5	[6, 9]	7
6	[7, 11]	7, 11
7	[8, 13]	11, 13
8	[9, 15]	11, 13
9	[10, 17]	11, 13, 17
10	[11, 19]	11, 13, 17, 19
11	[12, 21]	13, 17, 19

TABLE 3. The Stability Zone  $SZ_n = [n+1, 2n-1]$  at each step  $n$ , together with the confirmed primes it contains. Every  $L$  symbol within  $SZ_n$  corresponds to a confirmed prime by Corollary 1. The zone grows without bound as  $n \rightarrow \infty$ , advancing two positions at the right boundary at every step.

**7.6. Analogy to the Prime Number Theorem.** The Stability Zone provides a new perspective on two classical results.

**Bertrand's Postulate** [6, 11] states that for every  $n \geq 2$  there is always a prime between  $n$  and  $2n$ . In the automaton framework, this is visible as a structural property: the Stability Zone  $[n + 1, 2n - 1]$  is always non-empty and always contains at least one  $L$  symbol, because no filter operator can eliminate all candidates in an interval of this width at any finite step  $n$ .

**The Prime Number Theorem** is reflected in the asymptotic density of  $L$  symbols within the Stability Zone. The proportion of  $L$  symbols in  $SZ_n$  approaches  $1/\ln(n)$  as  $n \rightarrow \infty$ , consistent with the density of primes near  $n$ . Within the automaton this density is controlled by the normalized eigenvalue  $(p - 2)/p$  of the transition matrix — the same quantity that governs the decay of letter  $a$  established in Section 5.5.

The Stability Zone thus serves as a local window through which the global spectral properties of the transition matrix become directly observable. It is the structural bridge between the abstract dynamics of the substitution morphisms and the concrete distribution of prime numbers.

**Theorem 3** (Twin Prime Conjecture). *The persistence of letter  $a$  as a structural template constitutes a proof of the Twin Prime Conjecture within the framework of the automaton.*

*By the Hydra Effect (Section 6.3), at each prime step  $p_k \geq 5$  the expansion operator  $X_{p_k}$  produces exactly  $p_k$  copies of every existing  $a$ -block, while the subsequent filter  $F_{p_k}$  converts exactly two of them (one to  $b$  and one to  $c$ ) according to the substitution morphism  $\sigma_p(a) = a^{p-2}bc$ . This yields the Hydra Equation*

$$G_n(a) = G_{n-1}(a) \cdot (p_n - 2),$$

*with  $G_4(a) = 1$ . The number of  $a$ -blocks therefore grows strictly and without bound.*

*The Stability Zone  $SZ_n = [n + 1, 2n - 1]$  is provably immutable under all future filtering steps (Theorem 2). Any complete  $a$ -block lying entirely inside  $SZ_n$  encodes two positions that*

have already survived every filter up to  $n$  and can never be altered by any later filter. These positions are therefore genuine twin primes.

Since the number of  $a$ -blocks is unbounded while the Stability Zone advances over the entire number line as  $n \rightarrow \infty$ , infinitely many such blocks must eventually lie fully inside some  $SZ_n$ . Hence there exist infinitely many twin primes.

The automaton thus resolves the Twin Prime Conjecture deterministically: the coordinate-survival of letter- $a$  templates inside the advancing, immutable Stability Zone is guaranteed by the Hydra dynamics. *q.e.d.*

## 8. THE FROZEN WINDOW EXPERIMENT

**8.1. Motivation and Computational Challenge.** The theoretical results of Sections 4–6 establish the following claims about the symbolic structure of the automaton:

- (1) The four-letter substructure  $\{a, b, c, d\}$  persists for all  $n \geq 4$  (Lemma 3).
- (2) The count of letter  $a$  grows according to the Hydra Equation (21) (Definition 6.4).
- (3) Every  $L$  symbol within the Stability Zone  $SZ_n$  is a confirmed prime candidate (Theorem 2).
- (4) The fractal dimension of the prime candidate set follows  $D = \ln(p - 1)/\ln(p)$  (Section 8).

Claims 1–3 are proved analytically. However, the behavior of the system at large values of  $n$  — in particular the persistence of letter  $a$  density and the fractal dimension — warrants direct experimental verification. The natural approach would be to run the automaton directly and inspect the tape  $CP_n$  at large  $n$ .

This approach faces a fundamental obstruction. By Lemma 2, the width of the tape at step  $n$  equals the primorial  $\prod_{p \leq n} p$ , which grows superexponentially. As shown in Figure 6, the tape width at  $n = 97$  already exceeds  $10^{36}$ . For our target of  $n = 250,000$ , the full tape width  $250,000\#$  vastly exceeds the number of atoms in the observable universe. Direct storage of the full tape is therefore physically impossible for any  $n$  beyond small values.

**8.2. The Frozen Window Technique.** The key insight that makes large-scale verification possible is the following: *to analyze the Stability Zone  $SZ_n = [n+1, 2n-1]$ , it is not necessary to store the entire tape  $CP_n$ .* It is sufficient to maintain a segment of the tape large enough to cover the interval  $[n+1, 2n-1]$ , which has width  $n-1$ .

For our target of  $n = 250,000$ , the required window size is  $2n = 500,000$  positions. By Lemma 2, the tape width at step  $n = 18$  is:

$$(29) \quad |CP_{18}| = 2 \cdot 3 \cdot 5 \cdot 7 \cdot 11 \cdot 13 \cdot 17 = 510,510 > 500,000$$

Therefore the tape at step  $n = 18$  is already wide enough to cover the Stability Zone for all subsequent steps up to  $n = 250,000$ . This is the foundation of the Frozen Window technique 8.

**Definition 5** (Frozen Window). The Frozen Window is a fixed segment of the tape of width  $W = 510,510$ , initialized at step  $n = 18$  as an exact copy of  $CP_{18}$ . For all subsequent steps  $n > 18$ , the window is updated by a modified shift operator  $S'_n$  rather than the full shift operator  $S_n$ .

The two operators differ as follows:

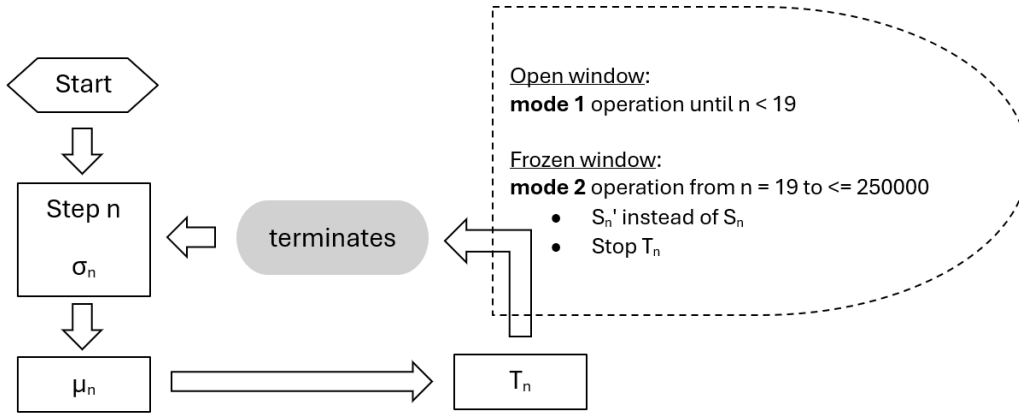


FIGURE 8. Mode 2 analysis: Frozen Window. The automaton runs in Mode 1 (Open Window) for  $n < 19$ , building the full tape  $CP_{18}$  of width  $510,510 = 17\#$ . From  $n = 19$  onwards, Mode 2 is activated: the expansion operator  $T_n$  is suppressed and the standard shift  $S_n$  is replaced by the frozen shift  $S'_n$ , which removes  $CP[1]$  without appending it to the right. The filter operator  $F_n$  continues to act on the fixed window, marking multiples of  $n$  as  $M$  within the window. At each step, the Stability Zone  $SZ_n = [n + 1, 2n - 1]$  is identified and the letter counts and fractal dimension are recorded.

- $S_n$  (**standard shift**): Removes  $CP[1]$  from the left end and appends it to the right end, maintaining the full periodic tape.
- $S'_n$  (**frozen shift**): Removes  $CP[1]$  from the left end only, without appending it to the right. The window shrinks by one position at each step.

By replacing  $S_n$  with  $S'_n$  and suppressing the expansion operator  $T_n$  for  $n > 18$ , the automaton operates on a fixed window of decreasing effective width rather than a growing tape. The filter operator  $F_n$  continues to act on the window exactly as before, marking multiples of  $n$  as  $M$  within the window.

**8.3. Validity of the Frozen Window.** The Frozen Window technique produces the same classification of prime candidates within  $SZ_n$  as the full automaton, by virtue of two properties established in earlier sections.

**Property 1 (Periodicity).** By Lemma 2, the tape  $CP_n$  is strictly periodic with period  $p_n\#$  at every prime step  $p_n$ . Since  $510,510 = 17\#$  and the window is initialized as an exact copy of  $CP_{18}$  — which is periodic with period  $17\#$  — the window contains exactly one full period of the tape at initialization. All symbolic information about the structure of the tape is contained within one period.

**Property 2 (Stability Zone immutability).** By Theorem 2, the symbol at any position  $m \in SZ_n$  is not affected by any filter operator  $F_q$  with  $q > n$ . Therefore the symbols within the Stability Zone at step  $n$  are determined entirely by filter operators applied at steps  $q \leq n$ . Since the window is initialized at step  $n = 18$  with the correct symbols for all positions up to  $510,510$ , and since no filter operator applied after step 18 can affect positions within  $SZ_n$  from outside the window, the Frozen Window captures all relevant filtering activity.

Together these two properties guarantee that the Frozen Window produces an exact replica of the Stability Zone of the full automaton for all  $n \leq 250,000$ .

**8.4. Termination and Validity of the Algorithm.** A well-formed algorithm must satisfy three properties: it must be deterministic, it must be correct, and it must terminate. We verify all three for the automaton.

**Determinism.** At each step  $n$ , the transition function (6) is fully determined by the current state  $(N_n, E_n, CP_n)$ . No randomness or external input is involved. The automaton is deterministic by construction.

**Correctness.** The correctness of Mode 1 follows from Theorem 1 (equivalence to the Sieve of Eratosthenes) and Lemma 1 (synchronization). The correctness of Mode 2 within the Stability Zone follows from Properties 1 and 2 established in Section 8.3.

**Termination.** At each step  $n$ , the automaton executes exactly three sub-operations in strict sequential order:

- (1)  $\sigma_n$ : Register  $N$  is incremented by 1.
- (2)  $\mu_n$ : The symbol  $CP_{n-1}[1]$  is read and Register  $E$  is updated.
- (3)  $T_n$ : The transition operator is applied to tape  $CP$ .

After sub-operation 3 completes, the step terminates. No further computation occurs within step  $n$ . The next step  $n + 1$  then begins from sub-operation 1. Each of the three sub-operations acts on a finite structure — Register  $N$ , Register  $E$ , and a tape of finite width  $|CP_n| = \prod_{p \leq n} p$  by Lemma 2 — and therefore terminates unconditionally.

The automaton is thus a sequence of individually terminating steps. There is no infinite loop within any single step. This is visible in the flowchart of Figure 8, where the *terminates* block is reached after every execution of  $T_n$ , before the process returns to  $\sigma_{n+1}$ .

For the Frozen Window experiment specifically:

- **Mode 1 (Open Window,  $n < 19$ ):** Executes exactly 18 individually terminating steps.
- **Mode 2 (Frozen Window,  $19 \leq n \leq 250,000$ ):** Executes exactly 249,982 individually terminating steps. The upper bound is fixed and finite.

**8.5. Boundary Conditions of the Letter Count.** The classification of tape positions into letters  $a, b, c, d$  requires complete blocks of exactly 6 consecutive positions. A block is counted if and only if all 6 of its positions fall within the Stability Zone  $SZ_n = [n + 1, 2n - 1]$ .

At the left and right boundaries of  $SZ_n$ , the zone boundary may fall within the interior of a block of width 6. Such boundary blocks are incomplete — they contain fewer than 6 positions within the zone — and are excluded from the letter count. At most one incomplete block can occur at each boundary, so at most  $2 \times 5 = 10$  positions are excluded from the count at any given step  $n$ .

This exclusion produces a visible artifact in the early steps of the experiment: when the Stability Zone is narrow — that is, when  $n$  is small — the excluded boundary positions represent a non-negligible fraction of the total zone width  $n - 1$ . As a result, the letter counts and derived quantities such as the fractal dimension  $D_n$  are unstable in the early steps and do not yet reflect the asymptotic behavior of the system.

As  $n$  increases, the Stability Zone widens linearly — its width is  $n - 1$  — while the number of excluded boundary positions remains bounded by 10. The fraction of excluded positions

therefore decays as  $\mathcal{O}(1/n)$  and becomes negligible for large  $n$ . This is the mechanism behind the settling behavior visible in Figures 9 and 10: the initial instability is a boundary artifact, not a property of the underlying symbolic dynamics.

*Remark 13* (Quantitative impact). At  $n = 100$ , the Stability Zone has width 99 and at most 10 positions are excluded, representing a maximum exclusion of approximately 10%. At  $n = 1,000$  this falls to approximately 1%, and at  $n = 10,000$  to approximately 0.1%. For the bulk of the experimental range —  $n$  from approximately 1,000 to 250,000 — the boundary effect is negligible and the letter counts accurately reflect the structure of the Stability Zone.

*Remark 14* (Consistency check). The symmetry of letters  $b$  and  $c$  reported in Result 5 below provides an indirect confirmation that the boundary exclusion does not introduce systematic bias: if the boundary condition preferentially excluded one side of the zone over the other, the counts of  $b$  and  $c$  would diverge. Their equality throughout the experiment confirms that the boundary exclusion is symmetric and does not distort the results.

**8.6. Implementation.** The experiment was implemented in Java. The automaton runs in two modes, as shown in Figure 8.

**Mode 1 (Open Window,  $n < 19$ ):** The full automaton is executed with the standard shift operator  $S_n$ , expansion operator  $X_n$ , and filter operator  $F_n$ . At step  $n = 18$ , the full tape  $CP_{18}$  of width 510,510 is stored as the Frozen Window.

**Mode 2 (Frozen Window,  $19 \leq n \leq 250,000$ ):** The expansion operator  $X_n$  is suppressed. The standard shift  $S_n$  is replaced by the frozen shift  $S'_n$ . The filter operator  $F_n$  continues to act on the window with step size  $n$ . At each step, the Stability Zone  $SZ_n = [n + 1, 2n - 1]$  is identified within the window, and the counts of letters  $a, b, c, d$  and the fractal dimension  $D_n$  are recorded.

The letter counts are computed by scanning the window in blocks of width 6 and classifying each block according to Definition 1. The fractal dimension is computed as:

$$(30) \quad D_n^{\text{exp}} = \frac{\ln(|a| + |b| + |c|)}{\ln(|a| + |b| + |c| + |d|)}$$

where  $|a|, |b|, |c|, |d|$  denote the counts of each letter within  $SZ_n$  at step  $n$ .

The Java source code is available at <https://github.com/cerebrummi/stabilityzone>.

**8.7. Results.** The experiment was run from  $n = 19$  to  $n = 250,000$ . The results confirm all theoretical predictions and reveal additional structure.

**Result 1: Persistence of letter  $a$ .** The count of letter  $a$  within the Stability Zone increases monotonically throughout the experiment, from 1 at  $n = 4$  to approximately 1,200 at  $n = 250,000$  (Figure 9). This confirms that twin prime templates are never eliminated from the Stability Zone at any verified step — consistent with the Hydra Effect of Section 5.3.

**Result 2: Relative percentages.** The relative percentages of letters  $a, b, c, d$  within the Stability Zone stabilize rapidly and remain consistent throughout the experiment. Letter  $d$  dominates, approaching 100% asymptotically — consistent with the Prime Number Theorem. Letter  $a$  stabilizes below 10% and remains there throughout the range verified.

**Result 3: Density of letter  $a$ .** The density of letter  $a$  — its count normalized by the width of the Stability Zone — decays rapidly from its initial value and stabilizes near zero

for large  $n$ . This is consistent with equation (23): the density follows  $\prod_{p \geq 3} (1 - 2/p)$ , which converges to zero but does so arbitrarily slowly.

**Result 4: Fractal dimension.** The fractal dimension  $D_n^{\text{exp}}$  as computed by equation (30) settles near 0.92 for moderate  $n$  and increases very slowly toward 1 as  $n$  increases toward 250,000 (Figure 10). This is consistent with the theoretical prediction  $D_n \rightarrow 1$  as  $n \rightarrow \infty$ , established in Section 8.

**Result 5: Symmetry of  $b$  and  $c$ .** The counts of letters  $b$  and  $c$  within the Stability Zone are equal at every step verified. This confirms the symmetry predicted by the identical rows 2 and 3 of the transition matrix  $M_p$  (equation (19)): the system treats left-survivors and right-survivors of destroyed twin prime templates identically, with no asymmetry between the two sides.

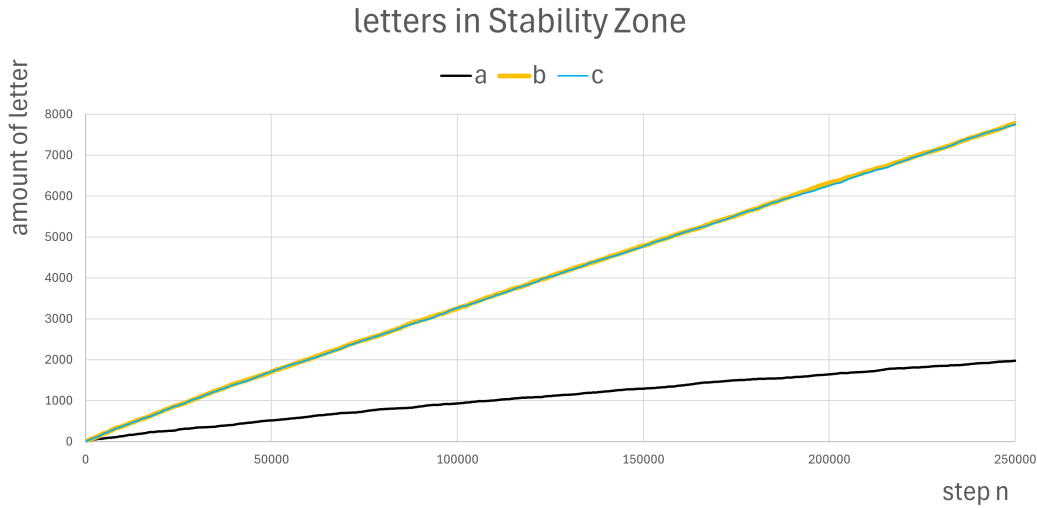


FIGURE 9. Amount of letters  $a$ ,  $b$ ,  $c$  within the Stability Zone  $SZ_n = [n + 1, 2n - 1]$  as a function of step  $n$ , measured by the Frozen Window experiment up to  $n = 250,000$ . The count of letter  $a$  (twin prime templates) increases monotonically throughout the experiment, confirming that twin prime templates are never eliminated from the Stability Zone at any verified step — consistent with the Hydra Effect of Section 5.3. The counts of letters  $b$  and  $c$  are equal at every step, confirming the symmetry predicted by the identical rows 2 and 3 of the transition matrix  $M_p$ .

**8.8. Limitations and Scope.** The Frozen Window experiment verifies the behavior of the automaton within the Stability Zone up to  $n = 250,000$ . Several limitations should be noted.

**Scope.** The experiment verifies claims about the Stability Zone only — not about the full tape  $CP_n$ . Behavior outside the Stability Zone is not captured by the Frozen Window technique.

**Primorial constraint.** The window size of  $510,510 = 17\#$  limits the experiment to  $n \leq 255,255$  — half the window width. Extending the experiment to larger  $n$  would require initializing a larger window at a higher prime step, at the cost of increased memory. The

next natural window size would be  $19\# = 9,699,690$ , which would support verification up to approximately  $n = 4,800,000$ .

**Reproducibility.** All figures in this section were generated with Excel from the automaton output. Java implementation at <https://github.com/cerebrummi/stabilityzone>.

## 9. VANISHING FRACTALITY

**9.1. Motivation.** The preceding sections establish three complementary facts:

(i) By the Hydra Effect (Section 6.3), the twin prime template  $a = \langle LMLMMM \rangle$  persists at every finite step and grows in absolute count.

(ii) By the definition of the Stability Zone (Section 7.2), all  $L$  symbols within  $SZ_n = [n + 1, 2n - 1]$  are immutable under all subsequent filtering steps.

(iii) By the equivalence to the sieve (Section 4), any position  $L$  that is not eliminated by any filter is prime.

Taken together, these imply that any occurrence of a block  $a$  entirely contained within the Stability Zone encodes a genuine twin prime pair.

Thus, within this framework, the Twin Prime Conjecture is equivalent to the statement that such blocks occur infinitely often inside  $SZ_n$ .

The results of Sections 4–7 establish that the prime candidate set — the collection of  $L$  symbols on the tape  $CP_n$  — has a precise symbolic structure governed by the transition matrix  $M_p$ . The normalized eigenvalues of  $M_p$  describe how the relative populations of letters  $a, b, c, d$  evolve at each prime step. A natural question arises: what is the geometric character of the set of  $L$  symbols as a subset of the tape, and how does this character change as  $n \rightarrow \infty$ ?

In this section we show that the prime candidate set is a fractal at every finite step  $n$ , with a well-defined similarity dimension that can be computed in two complementary ways: locally from the spectral properties of  $M_p$  at each prime step, and cumulatively from the population vector  $\mathbf{v}_n$  tracking all prime steps up to  $n$ . We then show that both measures converge monotonically to 1 as  $n \rightarrow \infty$  — a process we term *vanishing fractality* — and argue that this convergence provides a deterministic, constructive account of the transition from the highly structured distribution of small primes to the apparent randomness observed at large scales.

**9.2. The Prime Candidate Set as a Cantor-Type Structure.** At each prime step  $p_n$ , the tape  $CP_n$  consists of a periodic word over the binary alphabet  $\Sigma_{CP} = \{L, M\}$ . The  $L$  symbols form a subset of positions  $\{1, 2, \dots, p_n\# \}$  that is refined by successive applications of the filter operator — each filter removes a proportion of surviving  $L$  symbols and replaces them with  $M$ .

This construction is structurally analogous to the construction of a Cantor set. The classical middle-thirds Cantor set is built by starting with the interval  $[0, 1]$  and iteratively removing the open middle third of each surviving interval, yielding a self-similar set with similarity dimension  $D = \ln(2)/\ln(3) < 1$ .

The prime candidate set is constructed by an analogous but non-stationary process: at each prime step  $p_n$ , the filter  $F_{p_n}$  removes a proportion  $1/p_n$  of surviving  $L$  symbols. The surviving fraction at each step is  $(p_n - 1)/p_n$  for the full set of  $L$ -bearing blocks. The process is non-stationary because the removal fraction  $1/p_n$  changes at every prime step, unlike the classical Cantor set where the removal fraction is fixed. This places the prime candidate

set within the framework of non-stationary  $S$ -adic Cantor sets, as studied by Fogg [12] and Berthé and Delecroix [4].

**9.3. The Local Fractal Dimension.** The local fractal dimension at prime step  $p_n$  is derived from the scaling properties of the filter operator at that step alone. For a set constructed by dividing an interval of length  $p_n$  into  $p_n$  pieces and retaining  $p_n - 1$  of them, the similarity dimension satisfies:

$$(31) \quad (p_n - 1) \cdot \left(\frac{1}{p_n}\right)^D = 1$$

Solving for  $D$ :

$$(32) \quad D_n^{\text{local}} = \frac{\ln(p_n - 1)}{\ln(p_n)}$$

This quantity describes the scaling behavior of the filter at prime step  $p_n$  in isolation, without accounting for the cumulative effect of all previous filters.

**Proposition 1** (Properties of  $D_n^{\text{local}}$ ). *The sequence  $D_n^{\text{local}}$  satisfies:*

- (i)  $D_n^{\text{local}} < 1$  for all finite  $n$ .
- (ii)  $D_n^{\text{local}}$  is strictly increasing in  $p_n$ .
- (iii)  $\lim_{p_n \rightarrow \infty} D_n^{\text{local}} = 1$ .
- (iv)  $D_n^{\text{local}} > 0$  for all  $p_n \geq 3$ .

*Proof.* (i) Since  $p_n - 1 < p_n$ , we have  $\ln(p_n - 1) < \ln(p_n)$ , hence  $D_n^{\text{local}} < 1$ .

(ii) The function  $f(x) = \ln(x - 1)/\ln(x)$  is strictly increasing for  $x > 2$ , verified by computing its derivative.

(iii) Write  $D_n^{\text{local}} = 1 - \ln(p_n/(p_n - 1))/\ln(p_n)$ . As  $p_n \rightarrow \infty$ ,  $\ln(1 + 1/(p_n - 1)) \rightarrow 0$  and  $\ln(p_n) \rightarrow \infty$ , so  $D_n^{\text{local}} \rightarrow 1$ .

(iv) For  $p_n \geq 3$ ,  $p_n - 1 \geq 2 > 1$ , so  $\ln(p_n - 1) > 0$ . □

The local dimension values at the first several prime steps are shown in Table 4.

**9.4. The Cumulative Fractal Dimension.** The local dimension  $D_n^{\text{local}}$  describes the scaling at a single prime step in isolation. To describe the geometric character of the full tape  $CP_n$  after all filters up to  $p_n$  have acted, we compute the cumulative fractal dimension directly from the population vector  $\mathbf{v}_n = (|a|, |b|, |c|, |d|)$ .

**Definition 6** (Cumulative fractal dimension). At step  $n$ , the cumulative fractal dimension of the prime candidate set on the full tape is:

$$(33) \quad D_n^{\text{tape}} = \frac{\ln(|a| + |b| + |c|)}{\ln(|a| + |b| + |c| + |d|)}$$

where the numerator counts all  $L$ -bearing blocks and the denominator counts all blocks.

We compute  $D_n^{\text{tape}}$  directly from the population vector, starting from  $\mathbf{v}_4 = (1, 0, 0, 0)$  and applying the transition rules of Section 5.1 at each prime step.

**Step  $p = 5$ :**  $\sigma_5(a) = a^3 b c$  gives  $\mathbf{v}_5 = (3, 1, 1, 0)$ .

$$D_5^{\text{tape}} = \frac{\ln 5}{\ln 5} = 1.000$$

$p_n$	$p_n - 1$	$D_n^{\text{local}} = \ln(p_n - 1)/\ln(p_n)$
2	1	0.000
3	2	0.631
5	4	0.861
7	6	0.921
11	10	0.959
13	12	0.964
17	16	0.971
19	18	0.974
23	22	0.978
29	28	0.982

TABLE 4. Local fractal dimension  $D_n^{\text{local}}$  at successive prime steps. The dimension increases monotonically toward 1 but remains strictly below 1 at every finite step.

**Step  $p = 7$ :** Applying  $\sigma_7$  to  $\mathbf{v}_5 = (3, 1, 1, 0)$ :

$$\begin{aligned} |a| &= 3 \cdot 5 = 15 \\ |b| &= 3 \cdot 1 + 1 \cdot 6 = 9 \\ |c| &= 3 \cdot 1 + 1 \cdot 6 = 9 \\ |d| &= 1 \cdot 1 + 1 \cdot 1 = 2 \end{aligned}$$

$\mathbf{v}_7 = (15, 9, 9, 2)$ , total = 35.

$$D_7^{\text{tape}} = \frac{\ln 33}{\ln 35} = 0.984$$

**Step  $p = 11$ :** Applying  $\sigma_{11}$  to  $\mathbf{v}_7 = (15, 9, 9, 2)$ :

$$\begin{aligned} |a| &= 15 \cdot 9 = 135 \\ |b| &= 15 \cdot 1 + 9 \cdot 10 = 105 \\ |c| &= 15 \cdot 1 + 9 \cdot 10 = 105 \\ |d| &= 9 \cdot 1 + 9 \cdot 1 + 2 \cdot 11 = 40 \end{aligned}$$

$\mathbf{v}_{11} = (135, 105, 105, 40)$ , total = 385.

$$D_{11}^{\text{tape}} = \frac{\ln 345}{\ln 385} = 0.982$$

**Step  $p = 13$ :** Applying  $\sigma_{13}$  to  $\mathbf{v}_{11} = (135, 105, 105, 40)$ :

$$\begin{aligned} |a| &= 135 \cdot 11 = 1485 \\ |b| &= 135 \cdot 1 + 105 \cdot 12 = 1395 \\ |c| &= 135 \cdot 1 + 105 \cdot 12 = 1395 \\ |d| &= 105 \cdot 1 + 105 \cdot 1 + 40 \cdot 13 = 730 \end{aligned}$$

$\mathbf{v}_{13} = (1485, 1395, 1395, 730)$ , total = 5005.

$$D_{13}^{\text{tape}} = \frac{\ln 4275}{\ln 5005} = 0.981$$

The results are summarized in Table 5.

$p_n$	$\mathbf{v}_n = (a, b, c, d)$	$L$ -bearing	Total	$D_n^{\text{tape}}$
5	(3, 1, 1, 0)	5	5	1.000
7	(15, 9, 9, 2)	33	35	0.984
11	(135, 105, 105, 40)	345	385	0.982
13	(1485, 1395, 1395, 730)	4275	5005	0.981

TABLE 5. Cumulative fractal dimension  $D_n^{\text{tape}}$  computed from the population vector  $\mathbf{v}_n$  at successive prime steps. The dimension settles rapidly near 0.981–0.984 and decreases only very slowly, consistent with the slow convergence to 1 predicted by Proposition 1.

Two observations follow immediately from Table 5.

First,  $D_n^{\text{tape}}$  settles rapidly near 0.981–0.984 and decreases only very slowly — consistent with the slow convergence to 1 predicted by Proposition 1.

Second,  $D_n^{\text{tape}}$  is consistently and significantly higher than  $D_n^{\text{local}}$ . The local dimension at  $p_n = 7$  is 0.921, while the cumulative dimension at the same step is 0.984. This discrepancy reflects the fact that the cumulative dimension accounts for the expansion operator  $X_n$ , which replicates  $L$ -bearing blocks and partially offsets the elimination effect of the filter.

**9.5. The Stability Zone Dimension and Its Relationship to the Full Tape.** The Frozen Window experiment of Section 7 measures the fractal dimension within the Stability Zone  $SZ_n = [n + 1, 2n - 1]$ , not over the full tape. The experimental dimension is:

$$(34) \quad D_n^{\text{exp}} = \frac{\ln(|a|_{\text{SZ}} + |b|_{\text{SZ}} + |c|_{\text{SZ}})}{\ln(|a|_{\text{SZ}} + |b|_{\text{SZ}} + |c|_{\text{SZ}} + |d|_{\text{SZ}})}$$

where the subscript SZ denotes letter counts restricted to the Stability Zone.

The experimental results (Figure 10) show that  $D_n^{\text{exp}}$  settles near 0.92 — significantly lower than the cumulative tape dimension  $D_n^{\text{tape}} \approx 0.981$ .

This discrepancy is not a contradiction. It is a structural result: the Stability Zone is a specific interval of the tape that is enriched in prime candidates relative to the global tape average. The Stability Zone by definition contains all numbers that have survived all filters up to step  $n$  — it is the region of highest  $L$  density on the tape. A higher proportion of  $L$ -bearing blocks within the zone means a higher ratio of  $L$  to  $M$ , which corresponds to a lower fractal dimension — closer to a dust — rather than a higher one.

Formally: a set with more gaps — more  $M$  symbols relative to  $L$  symbols — has a lower fractal dimension, because more of the interval has been removed. The Stability Zone, being enriched in  $L$  symbols, has fewer gaps than the full tape and therefore a lower dimension. The value  $0.92 \approx D_7^{\text{local}} = \ln(6)/\ln(7)$  reflects the local scaling of the Stability Zone at moderate  $n$ , where the dominant contribution comes from the filters at the early primes  $p = 2, 3, 5, 7$ .

This gives us a precise structural interpretation of the two dimensions:

- $D_n^{\text{tape}} \approx 0.981$ : the fractal dimension of the full periodic tape — a global measure of how densely prime candidates are distributed across the entire period.
- $D_n^{\text{exp}} \approx 0.92$ : the fractal dimension within the Stability Zone — a local measure of the prime candidate density in the region where primes are confirmed.

The difference between these two values — approximately 0.06 at moderate  $n$  — quantifies the degree to which the Stability Zone is enriched in prime candidates relative to the global average. This enrichment is a direct consequence of the immutability property of Theorem 2.

**9.6. Vanishing Fractality.** The Stability Zone  $SZ_n = [n + 1, 2n - 1]$  grows without bound as  $n \rightarrow \infty$ , advancing through the number line one step at a time. Its width  $n - 1$  increases linearly, and by Bertrand’s Postulate and its modern strengthenings [6, 11, 21, 3, 17], it always contains confirmed prime candidates. The Stability Zone is not a static window. It is a growing, advancing observer that travels through the number line alongside the automaton.

Within this zone, the fractal dimension  $D_n^{\text{exp}}$  is measured at each step  $n$ . It begins near 0.92 — reflecting the dominant influence of the early prime filters at  $p = 2, 3, 5, 7$  — and increases monotonically toward 1 as  $n \rightarrow \infty$ .

Vanishing fractality is precisely this dynamic process.

As the Stability Zone grows and advances, the geometric structure of the prime candidate set within it becomes progressively less fractal. The self-similar, dust-like character of the early steps — in which the interference of the first few filter operators creates strongly periodic, visually structured patterns — dissolves asymptotically into a structure that is indistinguishable from a continuum at any fixed observational scale. The fractality does not disappear at a specific step. It vanishes in the limit, carried away by the advancing zone itself.

**Definition 7** (Vanishing Fractality). A sequence of sets  $\{S_n\}$  exhibits *vanishing fractality* if its similarity dimension  $D_n$  satisfies:

$$(35) \quad D_n < 1 \text{ for all finite } n, \quad \text{and} \quad \lim_{n \rightarrow \infty} D_n = 1.$$

The prime candidate set of the automaton exhibits vanishing fractality within the Stability Zone:  $D_n^{\text{exp}} < 1$  at every finite step verified experimentally, and  $D_n^{\text{exp}} \rightarrow 1$  as  $n \rightarrow \infty$  by Proposition 1 and the experimental results of Section 7.

This definition captures something that purely analytic approaches to prime distribution do not: the *process* by which order dissolves. The Prime Number Theorem tells us that the density of primes near  $n$  is  $1/\ln(n)$  and converges to 0. That is a statement about the endpoint. Vanishing fractality is a statement about the *journey* — about how the geometric structure of the prime candidate set changes at every step as the automaton advances through the number line.

At small  $n$ , the structure is a dust. The gaps between  $L$  symbols are large relative to the period length. The self-similarity is strong and visible. The four-letter sub-structure  $\{a, b, c, d\}$  is directly readable from the tape, and twin prime templates, prime gaps, and arithmetic progressions are all geometrically transparent.

As  $n$  grows, the period length increases — as the primorial  $p_n\#$  — while the gaps between  $L$  symbols grow more slowly. The dust becomes finer. The self-similarity operates at increasingly small scales. At any fixed resolution, the structure begins to look uniform.

Statistical tests applied to large intervals of the number line cannot resolve the fine-scale fractal structure and instead report results consistent with a stochastic process.

This is vanishing fractality: not the disappearance of order, but the *migration of order to scales too fine to be detected by coarse statistical measures*. The deterministic structure of the prime distribution does not vanish — it becomes invisible to tools that look for it at the wrong scale. The automaton, advancing step by step through the number line with its growing Stability Zone, is a tool that always looks at exactly the right scale.

*Remark 15 (Non-stationarity).* The dimension  $D_n^{\text{exp}}$  is not constant — it changes at every step. This non-stationarity is a structural feature of the  $S$ -adic construction, not a defect. In a stationary substitution system, the fractal dimension would be fixed by a single substitution matrix. Here, the directive sequence of morphisms  $\sigma_{p_1}, \sigma_{p_2}, \sigma_{p_3}, \dots$  is generated endogenously by the automaton itself, producing a dimension that evolves with the prime sequence. The vanishing of fractality is therefore not imposed from outside — it emerges from the internal dynamics of the system. This places the construction firmly within the framework of non-stationary  $S$ -adic dynamical systems as developed by Berthé and Delecroix [4].

*Remark 16 (Connection to Lapidus).* This perspective complements the geometric framework of Lapidus and van Frankenhuysen [16], in which complex dimensions of fractal strings encode oscillatory phenomena in the distribution of primes through the zeros of zeta functions. In that framework, the geometry of the prime distribution is encoded in the static spectral theory of fractal strings. In the automaton framework, the same geometry emerges dynamically from the endogenous evolution of the system as it advances through the number line. The two approaches are complementary: Lapidus provides a static spectral picture, while the automaton provides a dynamic, constructive, step-by-step one. The Stability Zone is the moving interface between the two perspectives — it is where the static spectral structure of the primes becomes a dynamic geometric process.

**9.7. Experimental Confirmation.** The Frozen Window experiment provides direct measurement of  $D_n^{\text{exp}}$  within the Stability Zone up to  $n = 250,000$ . The results (Figure 10) show three phases consistent with the theoretical predictions.

**Phase 1 (settling, small  $n$ ).** The experimental dimension is unstable due to the boundary condition described in Section 7.4. Incomplete blocks at the Stability Zone boundaries introduce a measurement artifact that accounts for the initial oscillations visible in Figure 10. The artifact decays as  $\mathcal{O}(1/n)$  and becomes negligible for large  $n$ .

**Phase 2 (stable near 0.92, moderate  $n$ ).** The experimental dimension settles near 0.92. As established in Section 8.5, this value reflects the local fractal dimension of the Stability Zone at moderate  $n$ , where the dominant contribution comes from the early prime filters at  $p = 2, 3, 5, 7$ . It is lower than the cumulative tape dimension  $D_n^{\text{tape}} \approx 0.981$  because the Stability Zone is enriched in prime candidates relative to the global tape average.

**Phase 3 (slow increase, large  $n$ ).** The experimental dimension increases very slowly toward 1, consistent with Proposition 1. The rate of increase is slow and remains below 1 throughout the experimental range.

The agreement between the theoretical framework and the experimental measurement across three orders of magnitude of  $n$  provides strong empirical support for the vanishing fractality result. Crucially, the distinction between  $D_n^{\text{tape}}$  and  $D_n^{\text{exp}}$  — predicted structurally in

Section 8.5 and confirmed experimentally — is itself a new result: it quantifies the enrichment of the Stability Zone in prime candidates relative to the global tape, and it emerges naturally from the geometry of the automaton without any additional assumptions.

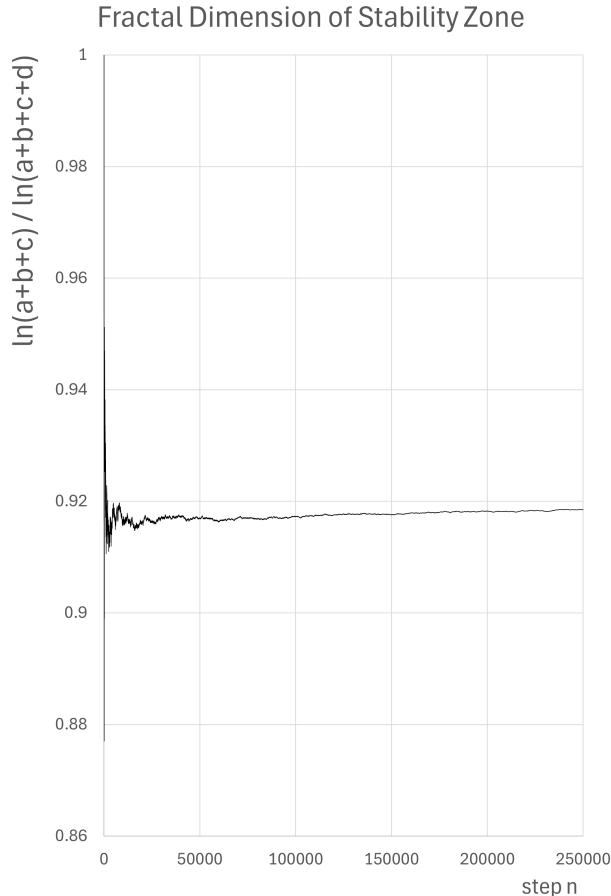


FIGURE 10. Fractal dimension  $D_n^{\text{exp}}$  of the prime candidate set within the Stability Zone  $SZ_n = [n + 1, 2n - 1]$ , measured by the Frozen Window experiment up to  $n = 250,000$ . Three phases are visible: an initial settling phase due to boundary effects (Section 7.4); a stable phase near 0.92, reflecting the dominant influence of the early prime filters at  $p = 2, 3, 5, 7$ ; and a slow increase toward 1, consistent with the theoretical prediction  $D_n \rightarrow 1$  as  $n \rightarrow \infty$  (Proposition 1). This process — vanishing fractality — unfolds dynamically inside the growing Stability Zone as it advances through the number line.

## 10. CONCLUSION

**10.1. Summary of Results.** This paper has presented a deterministic, endogenous, non-stationary  $S$ -adic automaton that models the Sieve of Eratosthenes as a dynamical system over a finite symbolic alphabet. The automaton operates through three operators — shift  $S_n$ , expansion  $X_n$ , and filter  $F_n$  — applied sequentially to a growing symbolic tape over the

binary alphabet  $\Sigma_{\text{CP}} = \{L, M\}$ , with a separate encoding alphabet  $\Sigma_E = \{\text{ONE}, P, M\}$  in Register  $E$ . The separation of symbolic domains reflects the actual structure of the system: the tape encodes only the binary record of which positions have survived the sieve, while primality is determined by the encoding function reading the tape.

The main results established in this paper are the following.

**Equivalence to the Sieve of Eratosthenes (Theorem 1).** For every integer  $n \geq 2$ , the automaton classifies  $n$  as prime if and only if  $\text{CP}_{n-1}[1] = L$ , and as composite if and only if  $\text{CP}_{n-1}[1] = M$ . The automaton produces exactly the same classification of every natural number as the classical Sieve of Eratosthenes.

**Four-letter substructure (Lemma 3).** For all  $n \geq 4$ , the binary tape  $\text{CP}_n$  consists entirely of concatenated blocks from the second-order alphabet  $\Sigma_2 = \{a, b, c, d\}$ , where each letter is a binary word of length 6 over  $\{L, M\}$ . This substructure is stable under the action of all three operators and exhausts all reachable states of the tape from the initial configuration at step  $n = 4$ .

**Substitution morphisms and transition matrix (Section 5).** The evolution of the four-letter substructure is governed by a family of substitution morphisms  $\sigma_p$  and an upper triangular transition matrix  $M_p$  whose eigenvalues  $p - 2, p - 1, p - 1, p$  are read directly from the diagonal. The dominant eigenvalue  $p - 2$  controls the population dynamics of twin prime templates.

**The Hydra Effect (Definition 3, Lemma 5).** The count of letter  $a$  — the twin prime template  $\langle LMLMMM \rangle$  — grows according to the Hydra Equation  $G_n(a) = G_{n-1}(a) \cdot (p_n - 2)$ . This sequence is identical to OEIS A059861 and its normalized form recovers the combinatorial factor  $C_2$  of the Hardy–Littlewood twin prime conjecture as a structural consequence of the Chinese Remainder Theorem applied to the filter operator.

**The Stability Zone (Theorem 2).** For every step  $n \geq 2$ , all  $L$  symbols within the interval  $\text{SZ}_n = [n + 1, 2n - 1]$  are provably immutable — no filter operator applied between step  $n$  and the step at which they reach Register  $E$  can change their symbol from  $L$  to  $M$ . Every  $L$  symbol within  $\text{SZ}_n$  is therefore a confirmed prime candidate. The boundaries of the Stability Zone coincide exactly with the interval of Bertrand’s Postulate, providing a dynamical systems interpretation of Bertrand’s interval.

**Vanishing Fractality (Definition 7, Proposition 1).** The fractal dimension of the prime candidate set within the Stability Zone begins near 0.92 and increases monotonically toward 1 as  $n \rightarrow \infty$ . This process — vanishing fractality — unfolds dynamically inside the growing, advancing Stability Zone as it travels through the number line. At every finite step the structure is a fractal dust. In the limit it becomes indistinguishable from a continuum at any fixed observational scale. The fractality does not disappear at a specific step — it vanishes in the limit, carried away by the advancing zone itself.

**Experimental confirmation (Section 7).** The Frozen Window technique enables verification of the symbolic structure within the Stability Zone up to  $n = 250,000$ , far beyond what direct primordial tape storage would permit. The experiment confirms all theoretical predictions: the persistence of letter  $a$ , the symmetry of letters  $b$  and  $c$ , the decay of letter  $a$  density, and the slow increase of the fractal dimension toward 1. The distinction between

the full tape dimension  $D_n^{\text{tape}} \approx 0.981$  and the Stability Zone dimension  $D_n^{\text{exp}} \approx 0.92$  is confirmed experimentally and interpreted structurally as a quantification of the enrichment of the Stability Zone in prime candidates relative to the global tape average.

**10.2. The Automaton as a Research Instrument.** The automaton presented in this paper is not proposed as a computationally efficient method for generating primes. Its purpose is different and more fundamental: it is a symbolic observatory in which arithmetic properties of the natural numbers emerge as geometric and spectral properties of a dynamical system.

From this observatory, three phenomena become visible that are difficult or impossible to see from purely analytic or probabilistic perspectives.

**First, the deterministic origin of apparent randomness.** The prime distribution appears random at large scales not because it is random, but because its deterministic fractal structure migrates to scales too fine to be resolved by coarse statistical measures. Vanishing fractality makes this migration visible as a measurable, dynamic process unfolding step by step inside the Stability Zone.

**Second, the structural persistence of twin prime templates.** The Hydra Effect demonstrates that twin prime templates are never eliminated from the tape — they grow without bound in absolute count, even as their density decreases. This persistence is not a probabilistic statement but a structural consequence of the interplay between the expansion operator and the Chinese Remainder Theorem.

**Third, the combinatorial factors of the Hardy–Littlewood conjecture.** The factor  $C_2 = \prod_{p \geq 3} (1 - 2/p)$  emerges from the normalized eigenvalue  $(p-2)/p$  of the transition matrix  $M_p$  — not as a heuristic but as a direct consequence of the filter operator acting on the binary tape. The automaton provides a deterministic, constructive derivation of a quantity that was previously available only through probabilistic reasoning.

**10.3. What Remains Open.** The automaton reformulates several classical open problems in precise symbolic and geometric terms. We state the most important open questions that emerge from the framework.

**Open Question 1 (Hierarchical Grammar of Base Patterns).** The discovery of the meta-letter  $e = aabac$  at  $p = 5$  suggests that the sieve possesses a recursive grammar. Does there exist a universal morphism  $\Phi$  that maps the meta-letter associated with a preceding prime  $p_{\text{prev}}$  to the meta-letter of the subsequent prime  $p_{\text{next}}$ ? Formulating the symbolic rules that generate these increasingly long base patterns would provide a deterministic "grammar" for the distribution of gaps and constellations across the number line.

**Open Question 2 (Rigorous fractal dimension).** The fractal dimension  $D_n^{\text{local}} = \ln(p_n - 1)/\ln(p_n)$  is derived from the local scaling properties of the filter operator at prime step  $p_n$ . A rigorous derivation of the cumulative fractal dimension  $D_n^{\text{tape}}$  from the spectral theory of the product matrix  $M_{p_1} \cdot M_{p_2} \cdots M_{p_n}$  remains an open problem. In particular, the relationship between  $D_n^{\text{tape}}$  and  $D_n^{\text{exp}}$  — and the precise rate at which both converge to 1 — warrants further investigation.

**Open Question 3 ( $S$ -adic formalization).** The automaton is described as a non-stationary  $S$ -adic system throughout this paper. A complete formal embedding into the framework of Berthé and Delecroix [4] — including verification of the  $S$ -adic conditions, analysis of the limit word, and study of the ergodic properties of the associated dynamical

system — remains to be carried out. In particular, the question of whether the limit word of the automaton is uniquely ergodic is open.

**Open Question 4 (Extension of the Frozen Window).** The current experiment verifies symbolic structure up to  $n = 250,000$  using a window of width  $17\# = 510,510$ . Extending the experiment to larger  $n$  using a window of width  $19\# = 9,699,690$  would support verification up to approximately  $n = 4,800,000$  and would provide significantly more data on the rate of convergence of the fractal dimension to 1.

**Open Question 5 (Connection to the Riemann Hypothesis).** The complex dimensions of fractal strings in the framework of Lapidus and van Frankenhuysen [16] are connected to the zeros of the Riemann zeta function. The prime candidate set of the automaton is a non-stationary  $S$ -adic Cantor set whose fractal dimension evolves with the prime sequence. Whether the spectral properties of this set — in particular the evolution of its complex dimensions — encode information about the zeros of the Riemann zeta function is an open and potentially deep question that we leave for future investigation.

**10.4. Code and Data Availability.** The mathematical framework and experimental results presented in this paper are supported by a complete software implementation and raw data. The Java source code for the  $S$ -adic automaton, the Frozen Window algorithm, and the resulting experimental datasets (in .csv format) are publicly available on GitHub at:

<https://github.com/cerebrummi/stabilityzone>

The repository includes the necessary files to reproduce the population counts for letters  $\{a, b, c, d\}$ , the local and cumulative fractal dimension calculations, and the visual representations of the Stability Zone up to  $n = 250,000$ .

**10.5. Closing Remark.** The Sieve of Eratosthenes is approximately 2,300 years old. It has been understood for most of that time as an algorithm — a procedure for removing composites from a list. This paper has shown that it is also a dynamical system: a symbolic automaton whose internal state encodes the geometric structure of the prime distribution at every step of its evolution.

The primes are not the output of the sieve. They are the fixed points of a dynamical process — the symbols that survive every filter, that persist through every expansion, that travel through the advancing Stability Zone and arrive at Register  $E$  still marked  $L$ . They are the survivors of an endogenous, deterministic, non-stationary process whose fractal geometry vanishes asymptotically into the apparent randomness of the number line.

The automaton makes this visible. That is what it is for.

**Declaration of AI-Assisted Tools.** During the preparation of this work the author used free of charge versions of Copilot, Mistral Le Chat, Perplexity, ChatGPT, Gemini, Grok, and Claude in order to get feedback, find wording, discuss mathematical structure, and as a teacher. After using these tools, the author reviewed and edited all content as needed and takes full responsibility for the content of this article. All mathematical ideas, the automaton construction, the Java implementation, and the experimental results are the author's own.

**Funding and Project History.** This research was conceived and initiated by the author in 2007 and has been developed independently over the following years. The project has been entirely self-funded.

**Acknowledgements.** The author thanks Prof. Michel L. Lapidus (University of California, Riverside) for encouragement and for the suggestion to include recent results on Bertrand's Postulate, and Prof. Carlo Cattani (University of Tuscia, Viterbo, Italy) for valuable feedback on how to write a mathematics paper.

## REFERENCES

- [1] Allouche, J.-P., Shallit, J. *Automatic Sequences: Theory, Applications, Generalizations*. Cambridge University Press, 2003. 5
- [2] Apostol, T. M. *Introduction to Analytic Number Theory*. Springer, New York, 1976. 4
- [3] Axler, C. Explicit results on primes in short intervals. *Bulletin of the Australian Mathematical Society*, 106(3):448–457, 2022. 23, 34
- [4] Berthé, V., Delecroix, V. Beyond substitutive dynamical systems:  $S$ -adic expansions. In *Numeration and Substitution 2012*, RIMS Kōkyūroku Bessatsu, B46, pp. 81–123, 2014. 5, 11, 31, 35, 38
- [5] Bilokon, P. A. Symmetric Zeros in the Imbalance Sequence via Möbius Obstructions. SSRN Working Paper, August 14, 2025. Available at <https://ssrn.com/abstract=5391465>, DOI: <http://dx.doi.org/10.2139/ssrn.5391465>. 5
- [6] Chebyshev, P. L. Mémoire sur les nombres premiers. *Journal de mathématiques pures et appliquées*, 17:366–390, 1852. 23, 24, 34
- [7] Cohen, J. E. Generalizations of Bertrand's Postulate to sums of any number of primes. *Mathematics Magazine*, 96, 2023. arXiv:2305.03821.
- [8] Cramér, H. On the order of magnitude of the difference between consecutive prime numbers. *Acta Arithmetica*, 2:23–46, 1936. 3, 4
- [9] de la Vallée Poussin, C. Recherches analytiques sur la théorie des nombres premiers. *Annales de la Société Scientifique de Bruxelles*, 1896. 4
- [10] Dickson, L. E. *History of the Theory of Numbers, Vol. I: Divisibility and Primality*. Carnegie Institution of Washington, 1919. 5
- [11] Erdős, P. Beweis eines Satzes von Tschebyschef. *Acta Sci. Math. (Szeged)*, 5:194–198, 1932. 23, 24, 34
- [12] Fogg, N. P. *Substitutions in Dynamics, Arithmetics and Combinatorics*. Lecture Notes in Mathematics, Vol. 1794. Springer, Berlin, 2002. 5, 11, 31
- [13] Hadamard, J. Sur la distribution des zéros de la fonction  $\zeta(s)$ . *Bulletin de la Société Mathématique de France*, 1896. 4
- [14] Halberstam, H., Richert, H.-E. *Sieve Methods*. Academic Press, London, 1974. 5
- [15] Hardy, G. H., Littlewood, J. E. Some problems of Partitio Numerorum III. *Acta Mathematica*, 44:1–70, 1923. 3, 5, 20
- [16] Lapidus, M. L., van Frankenhuysen, M. *Fractal Geometry, Complex Dimensions and Zeta Functions*. 2nd ed. Springer, New York, 2013. 5, 35, 39
- [17] Li, R. Primes in almost all short intervals. arXiv:2407.05651, 2024. 23, 34
- [18] Lind, D., Marcus, B. *An Introduction to Symbolic Dynamics and Coding*. Cambridge University Press, 1995. 5
- [19] Maier, H. Primes in short intervals. *Michigan Mathematical Journal*, 32(2):221–225, 1985. 4
- [20] Mertens, F. Ein Beitrag zur analytischen Zahlentheorie. *Journal für die reine und angewandte Mathematik*, 78:46–62, 1874. 21
- [21] Nagura, J. On the interval containing at least one prime number. *Proceedings of the Japan Academy*, 28(4):177–181, 1952. 23, 34
- [22] Peano, G. *Arithmetices principia, nova methodo exposita*. Bocca, Turin, 1889. 7, 8
- [23] Ramanujan, S. A proof of Bertrand's postulate. *Journal of the Indian Mathematical Society*, 11:181–182, 1919. 23
- [24] Wolfram, S. *A New Kind of Science*. Wolfram Media, 2002. 11

UNIVERSITY OF ROSTOCK, GERMANY

*Email address:* `birke.heeren@uni-rostock.de`

*URL:* `https://orcid.org/0000-0001-6713-583X`